3D Near-infrared Imaging Based on a Single-photon Avalanche Diode Sensor

Juan Mata Pavia

Cristiano Niclass

Martin Wolf

Edoardo Charbon

ÉCOLE POLYTECHNIQUE FÉDÉRALE DE LAUSANNE

BORL Biomedical Optics Research Laboratory
University Hospital Zurich | Clinic of Neonatology

UniversitätsSpital Zürich
Dept. Frauenheilkunde
Klinik für Neonatologie

Experimental Techniques

Continuous wave (CW)

Frequency domain (FD)

Time domain (TD)

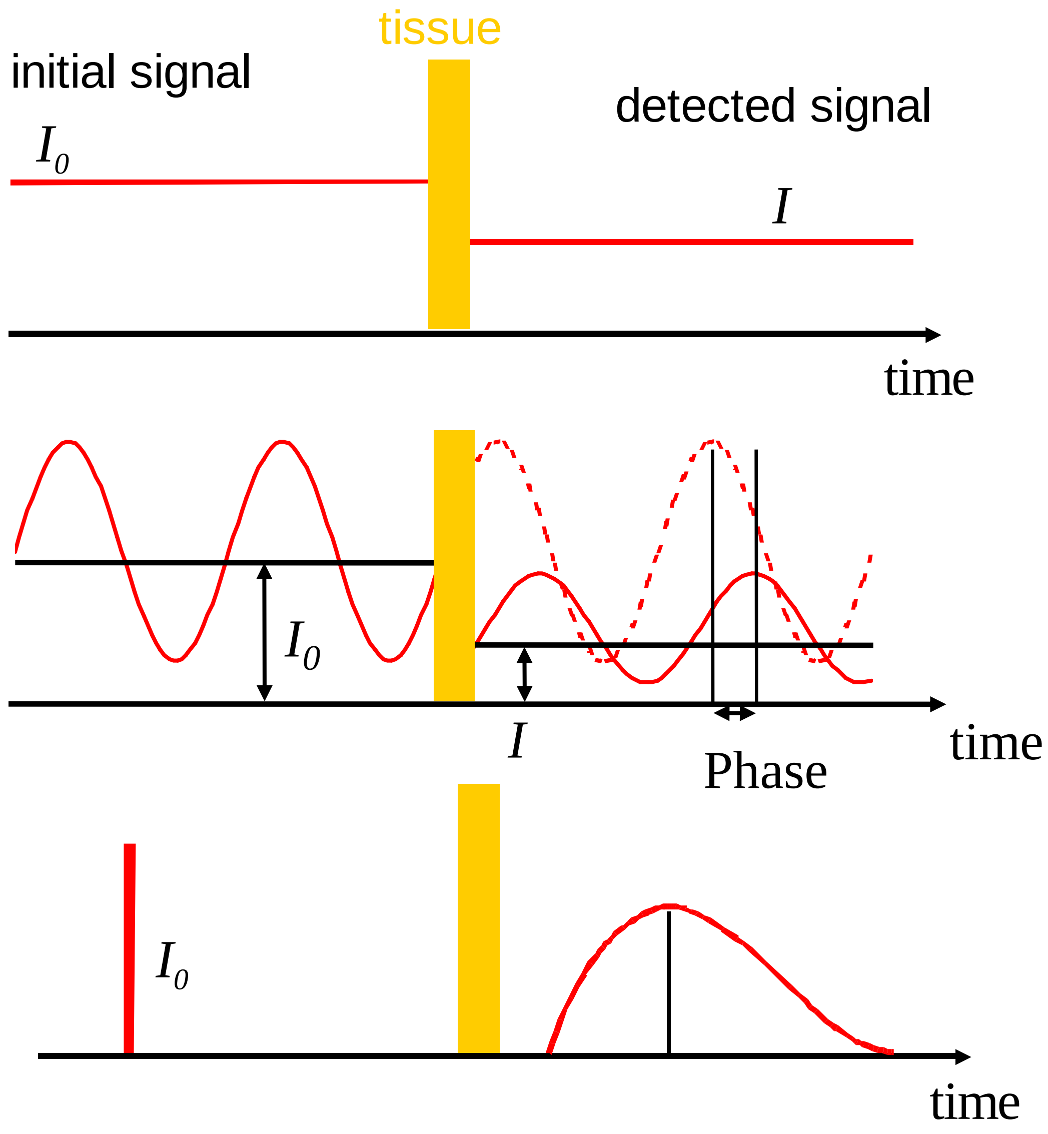

Near Infrared Imaging (NIRI)

- Low spatial resolution (~1cm resolution)
- 3D images require long acquisition times
- CW systems can be miniaturized
- TD and FD systems are bulky
- Low number of sources/detectors

[Muehlemann T *et al* Opt. Express 2008]

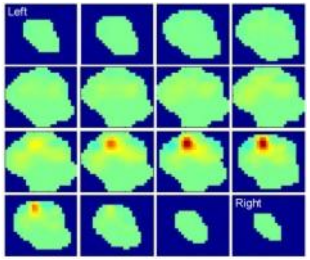

[Wells K *et al* Proc. SPIE 1997]

Single-photon avalanche diode (SPAD)

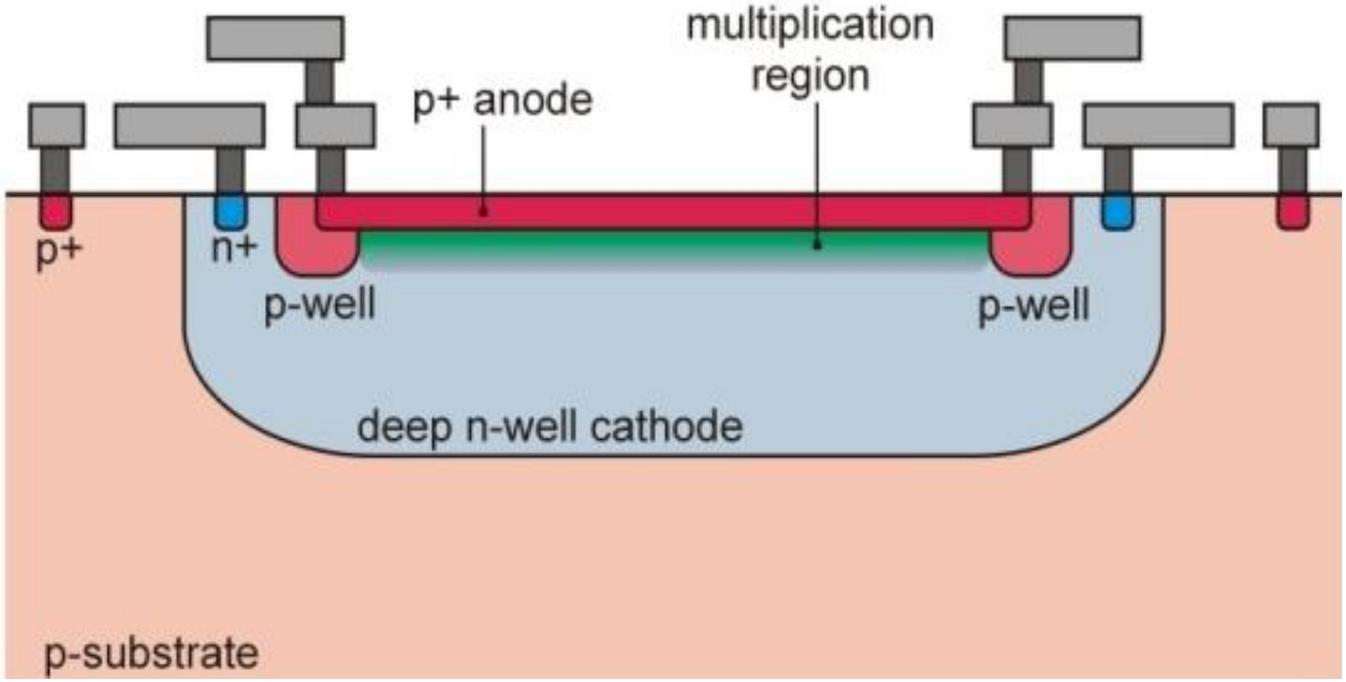

Objective

- New 3D NIRI system:
  - High resolution images: <1cm
  - Almost real time operation
  - Bedside applicable
- SPAD imagers offer:
  - High resolution images
  - Time resolved measurements

SPAD Image Sensor: LASP Chip

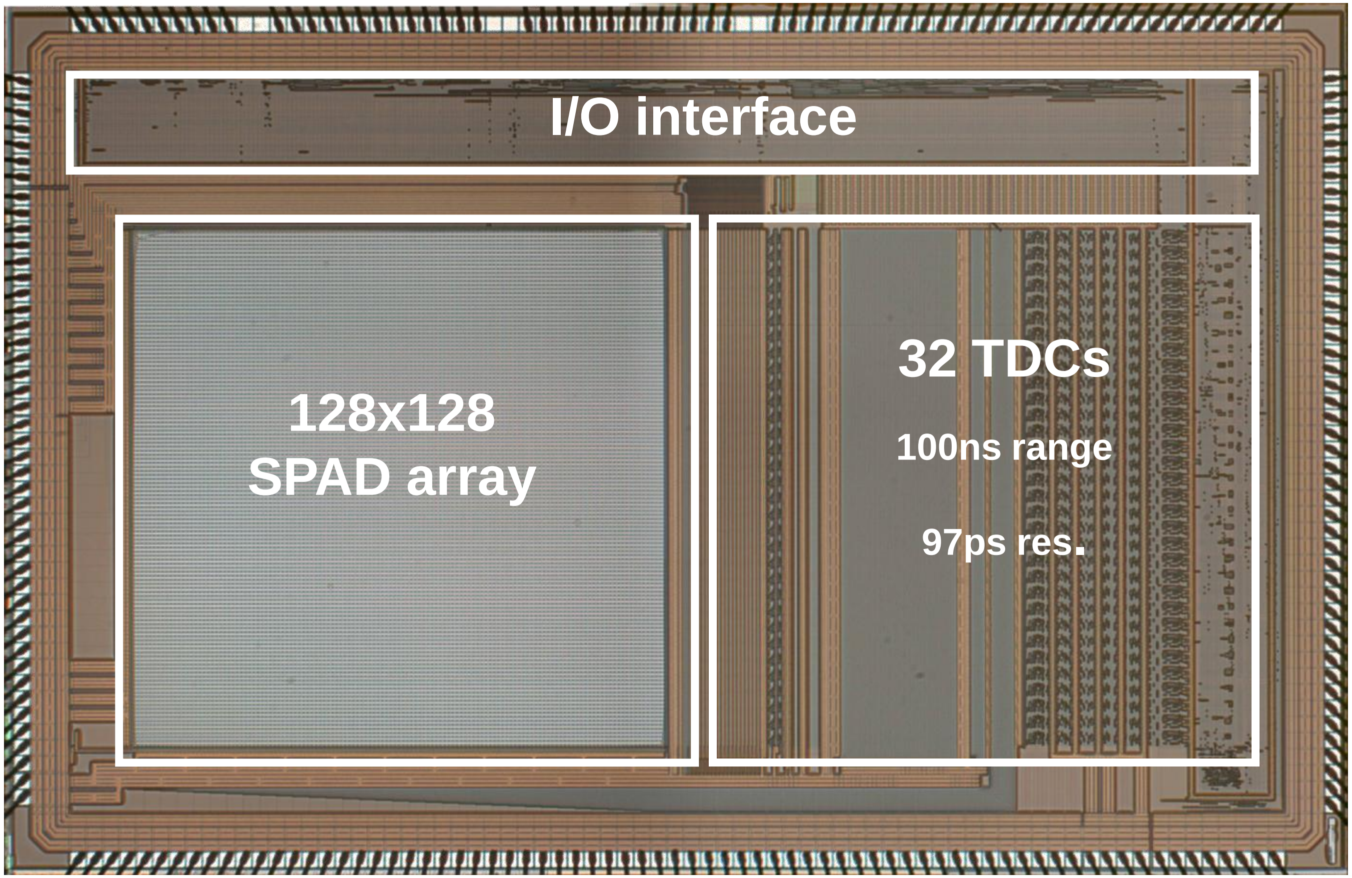

[Niclass *et al* JSSC 2008]

Experimental Setup with Cylindrical Waves I

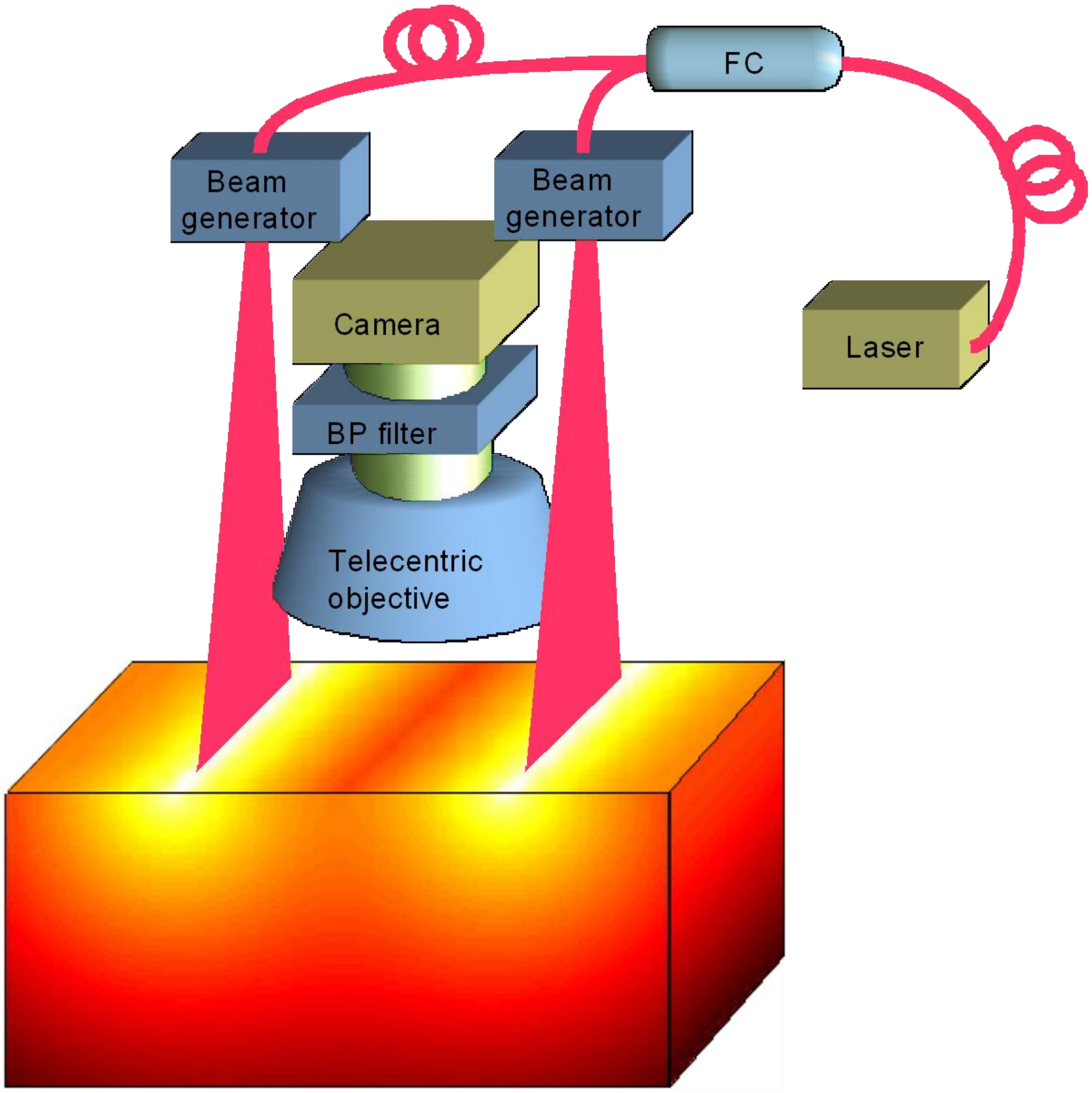

Experimental Setup with Cylindrical Waves II

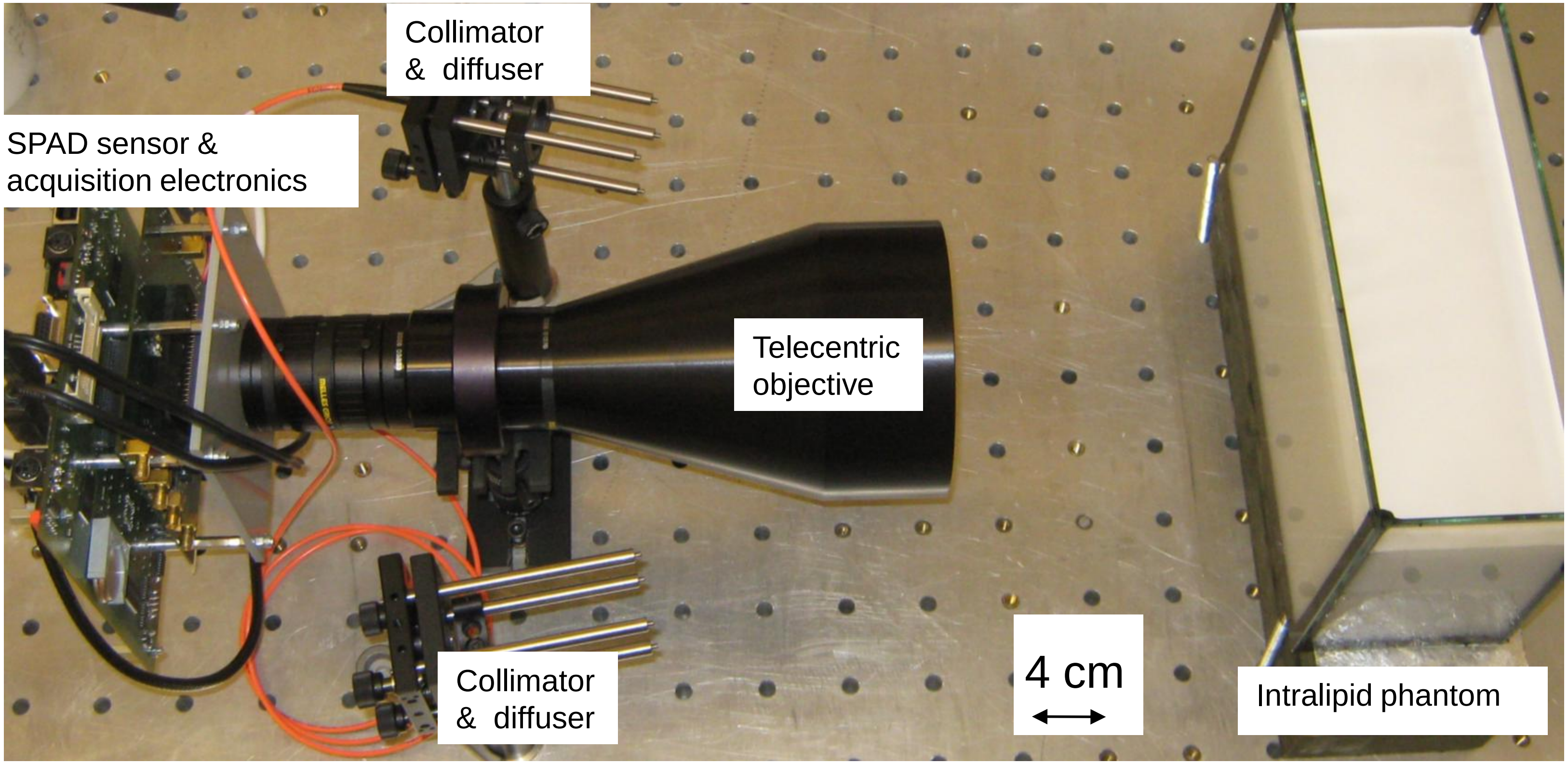

Phantom Measurements I

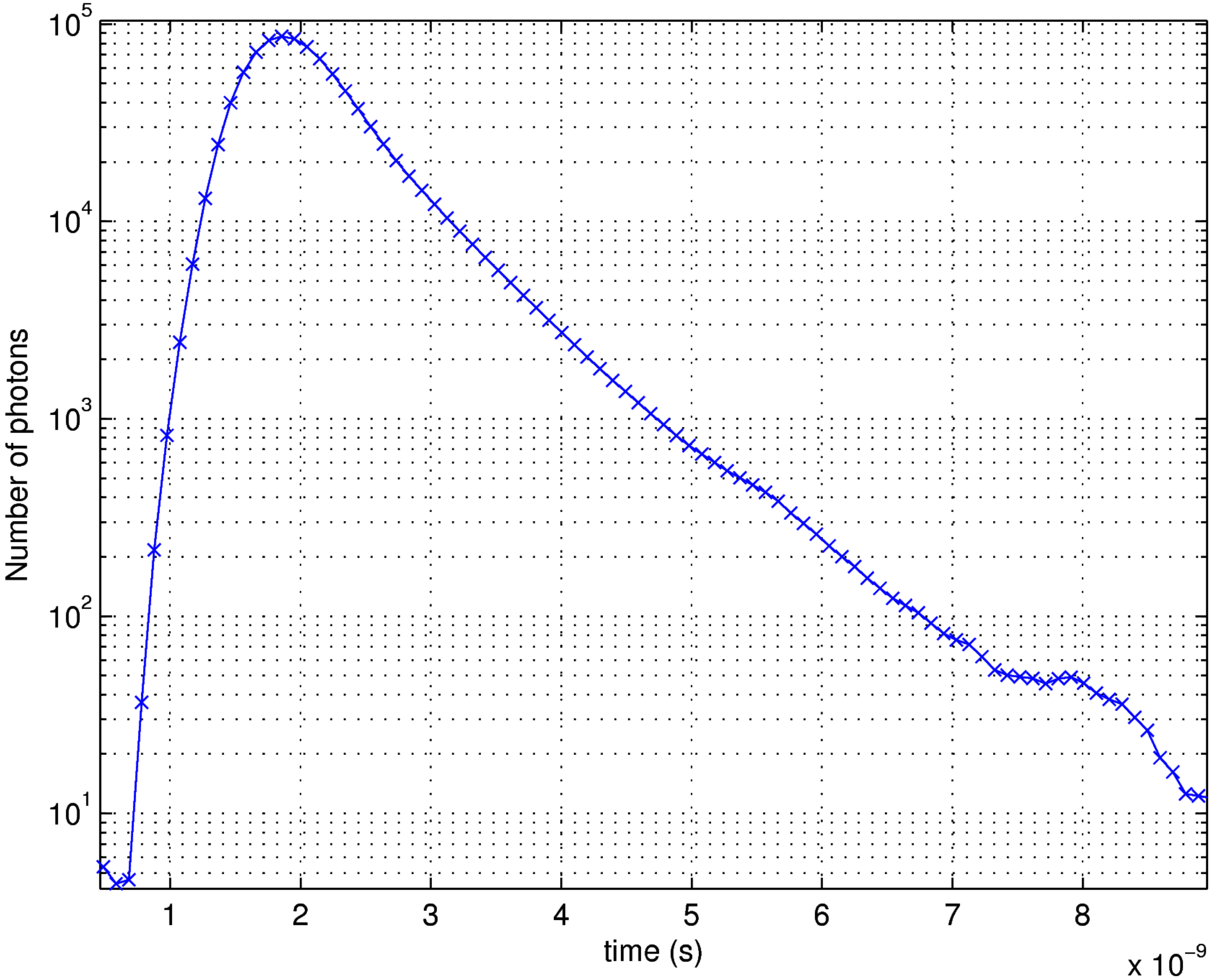

Phantom Measurements II

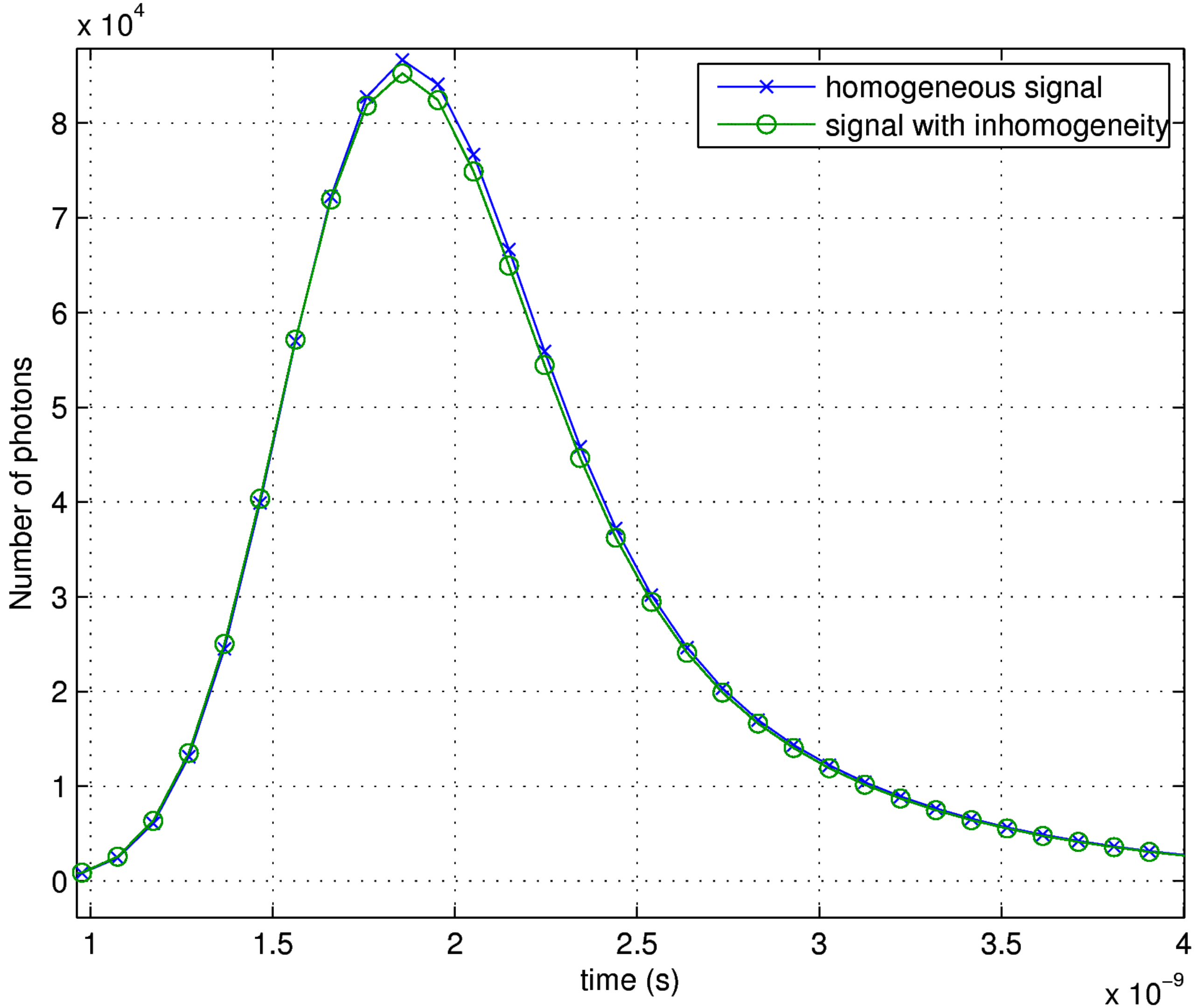

The Diffusion Equation

- Homogeneous medium
- Fourier in the time domain
- Born approximation

Object to be reconstructed

$$U_s(\vec{r},\omega_t) = -\iiint G(\vec{r},\vec{r}\,',\omega_t)\, O(\vec{r}\,')\, U_0(\vec{r}\,',\omega_t)\, d\vec{r}\,'$$

Measurement

Matrix coefficients

Object to be reconstructed

$$(\nabla^2 + k^2)\, U_s(\vec{r},\omega_t) = O(\vec{r})\, U_0(\vec{r},\omega_t)$$

Photon density in the homogeneous medium

Measurement

Fourier in the X dimension

$$(\nabla_{yz}^2 + k^2 - w_x^2)\, U_s(\vec{r}_{yz},\omega_x,\omega_t) = F_x\{O(\vec{r})\, U_0(\vec{r},\omega_t)\}$$

X independent

The triple integral is reduced to a double integral

$$U_s(\vec{r}_{yz},\omega_x,\omega_t) = -\iint G(\vec{r}_{yz},\vec{r}\,'_{yz},\omega_x,\omega_t)\, O(\vec{r}\,'_{yz},\omega_x)\, U_0(\vec{r}\,'_{yz},\omega_t)\, d\vec{r}\,'_{yz}$$

Experimental Results: Setup 1

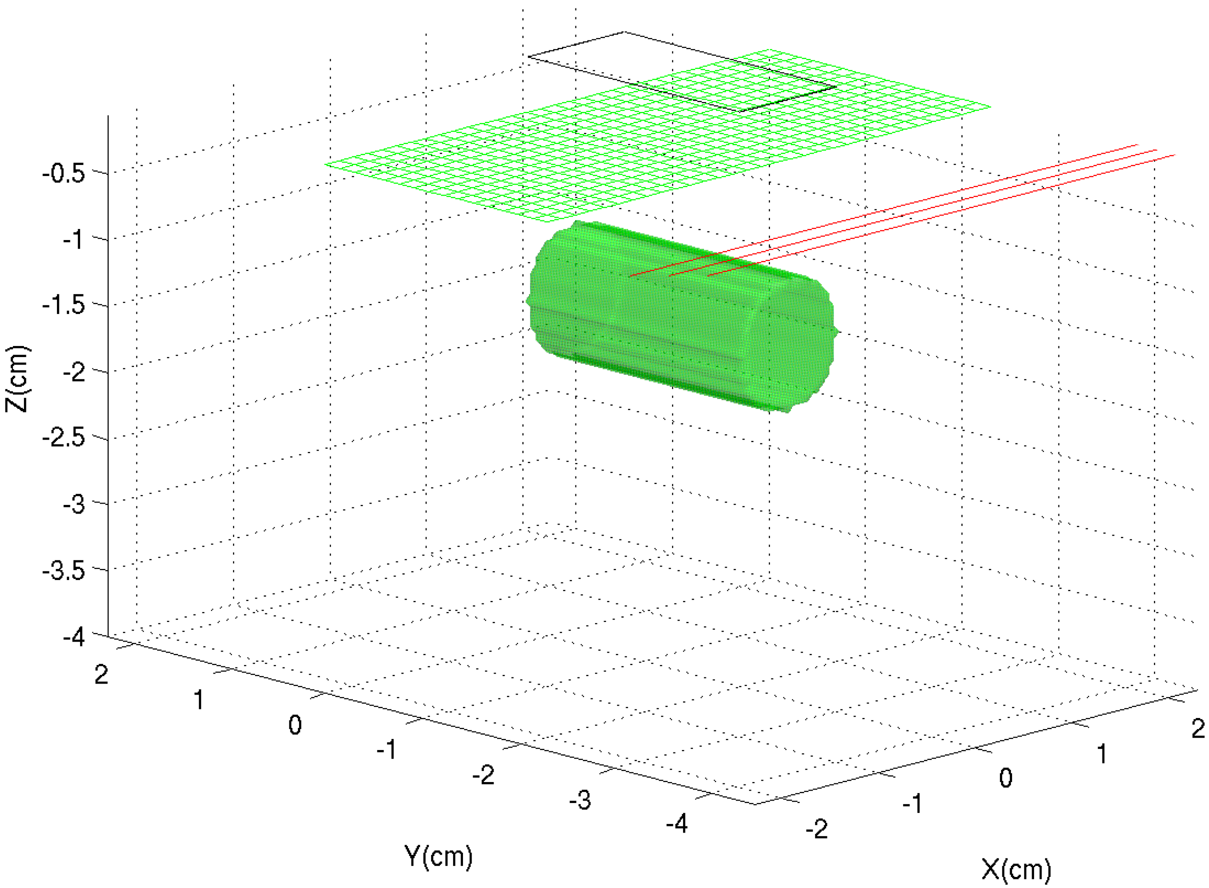

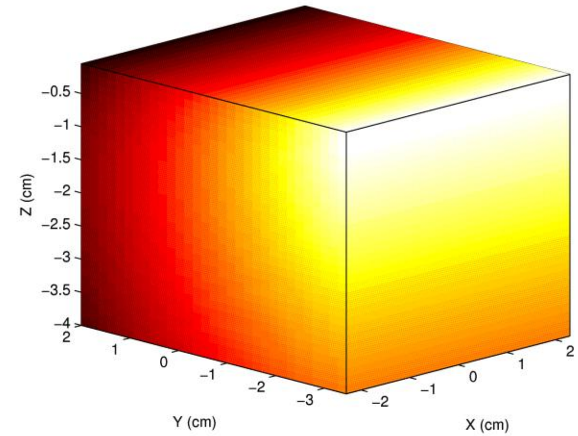

Experimental Results: Reconstruction 1

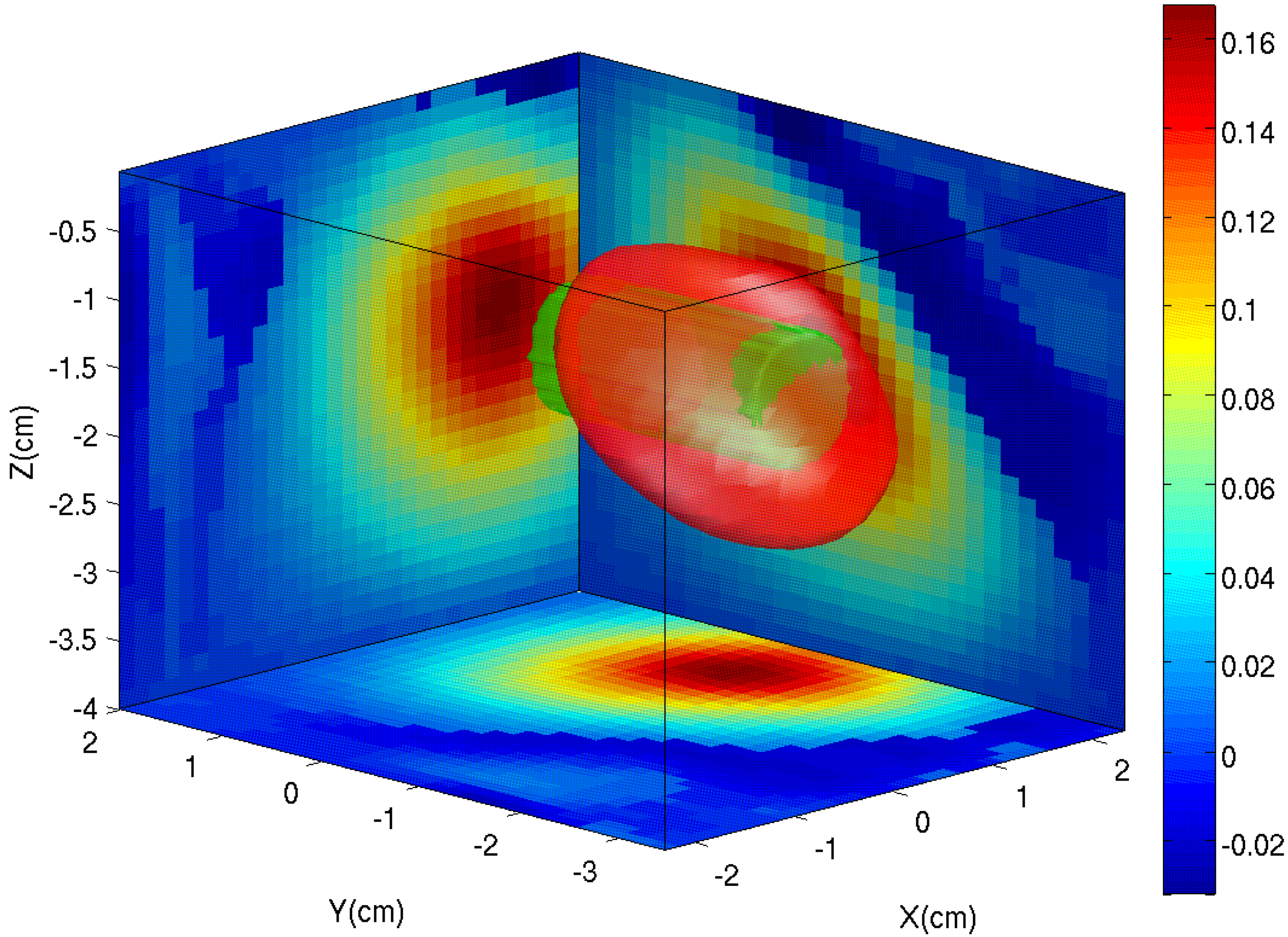

Experimental Results: Setup 2

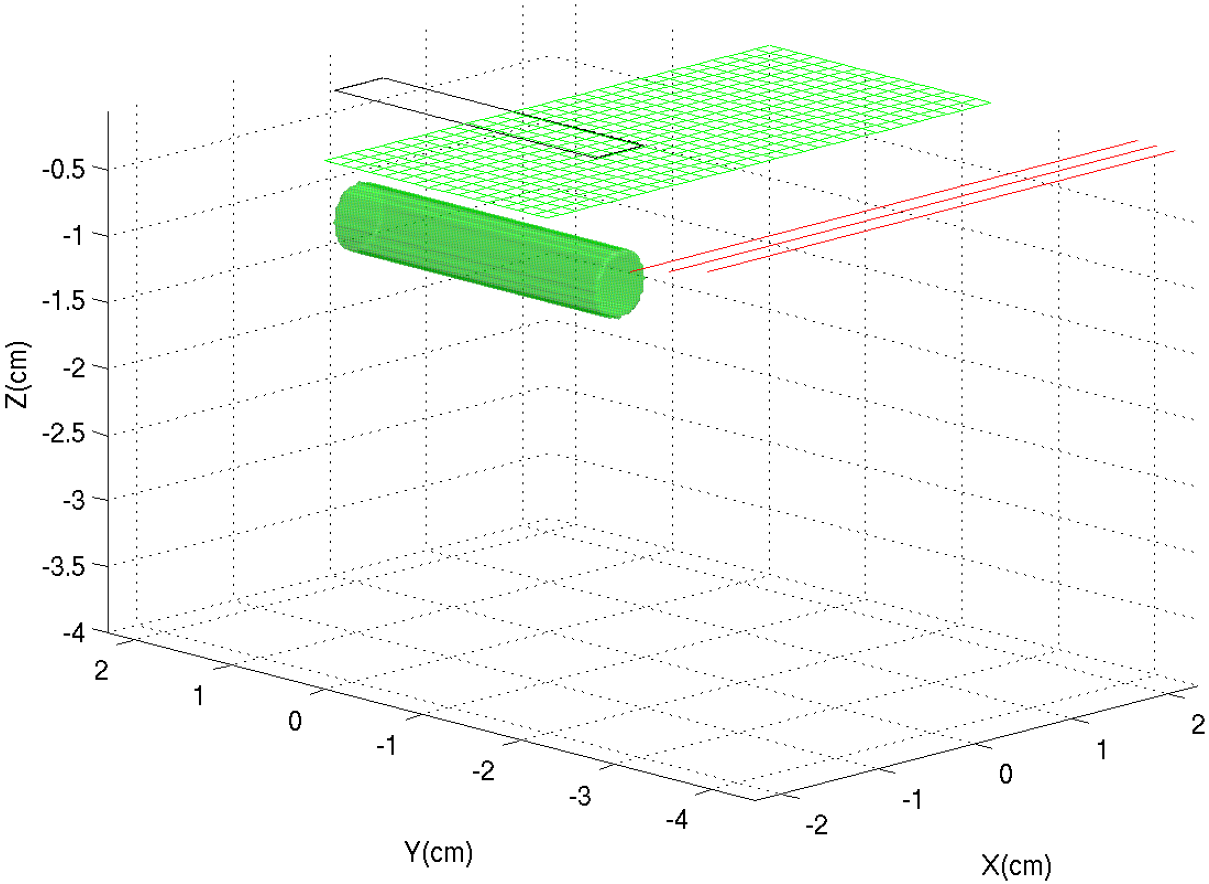

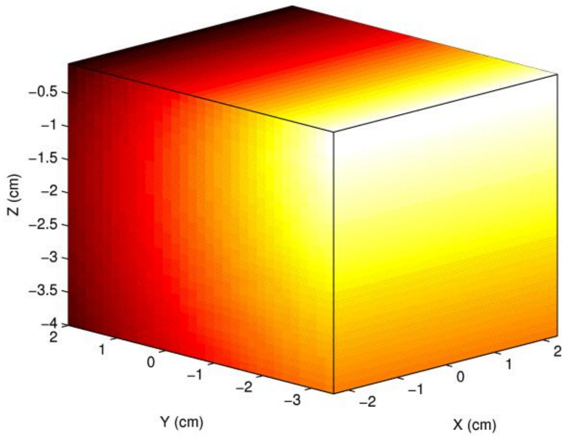

Experimental Results: Reconstruction 2

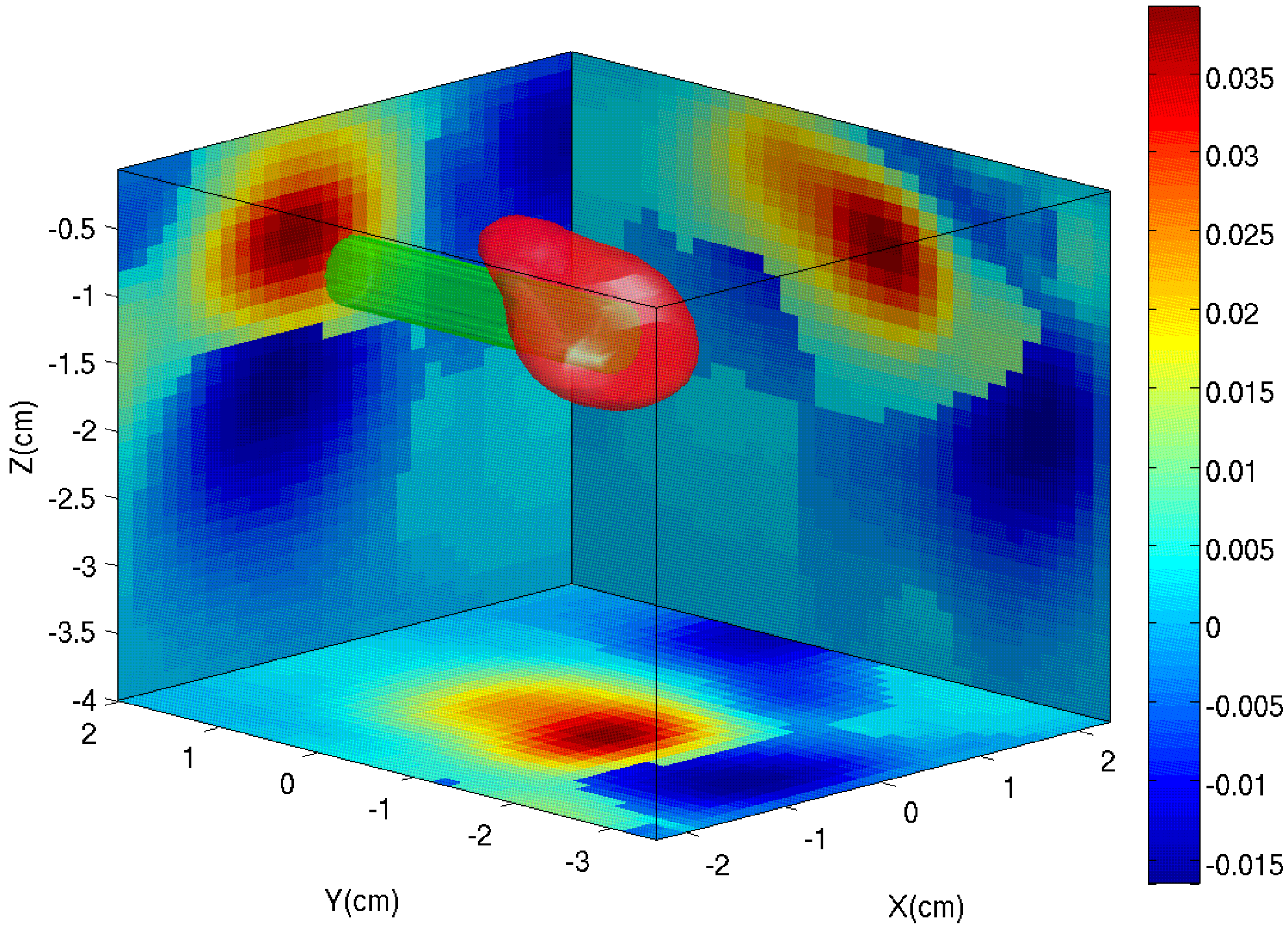

Experimental Results: Setup 3

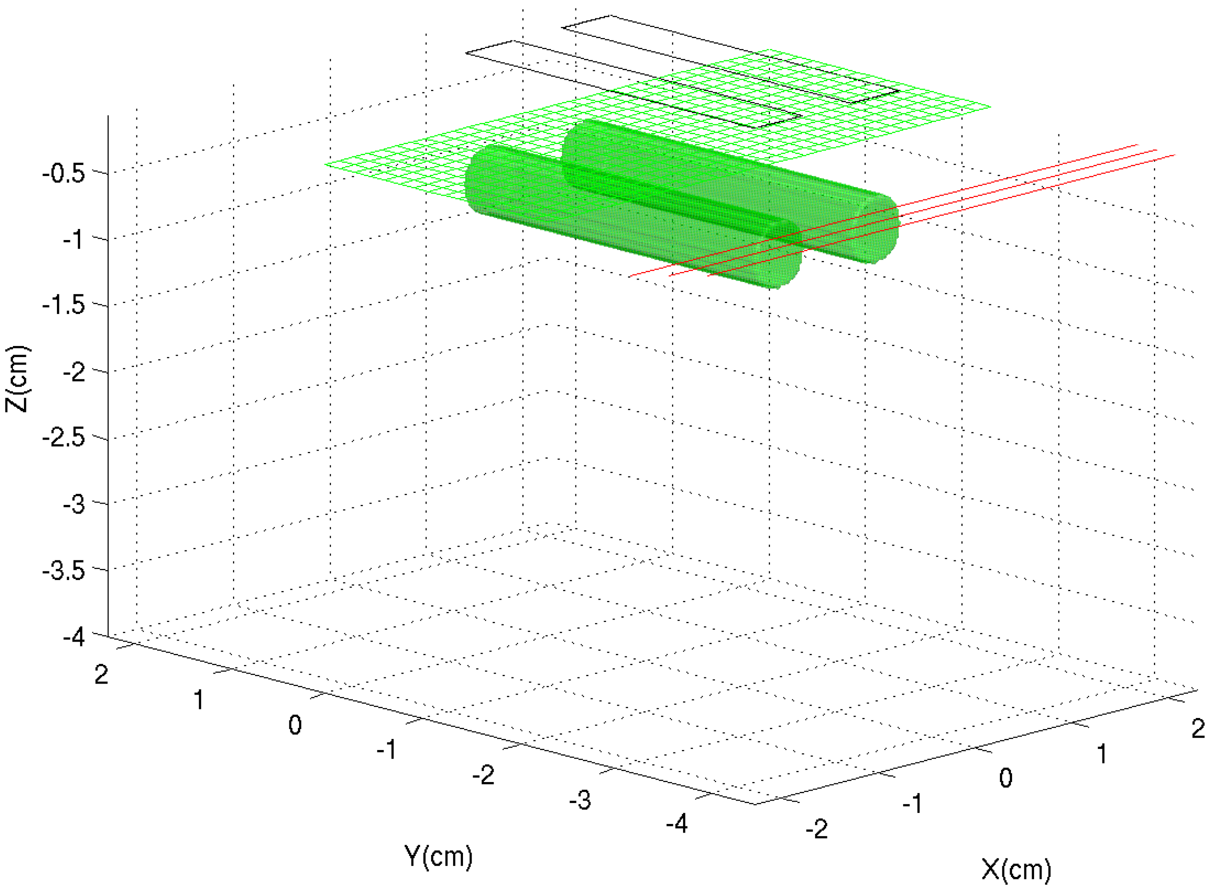

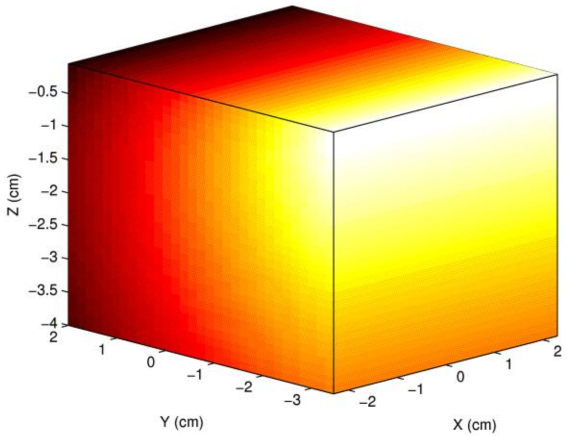

Experimental Results: Reconstruction 3

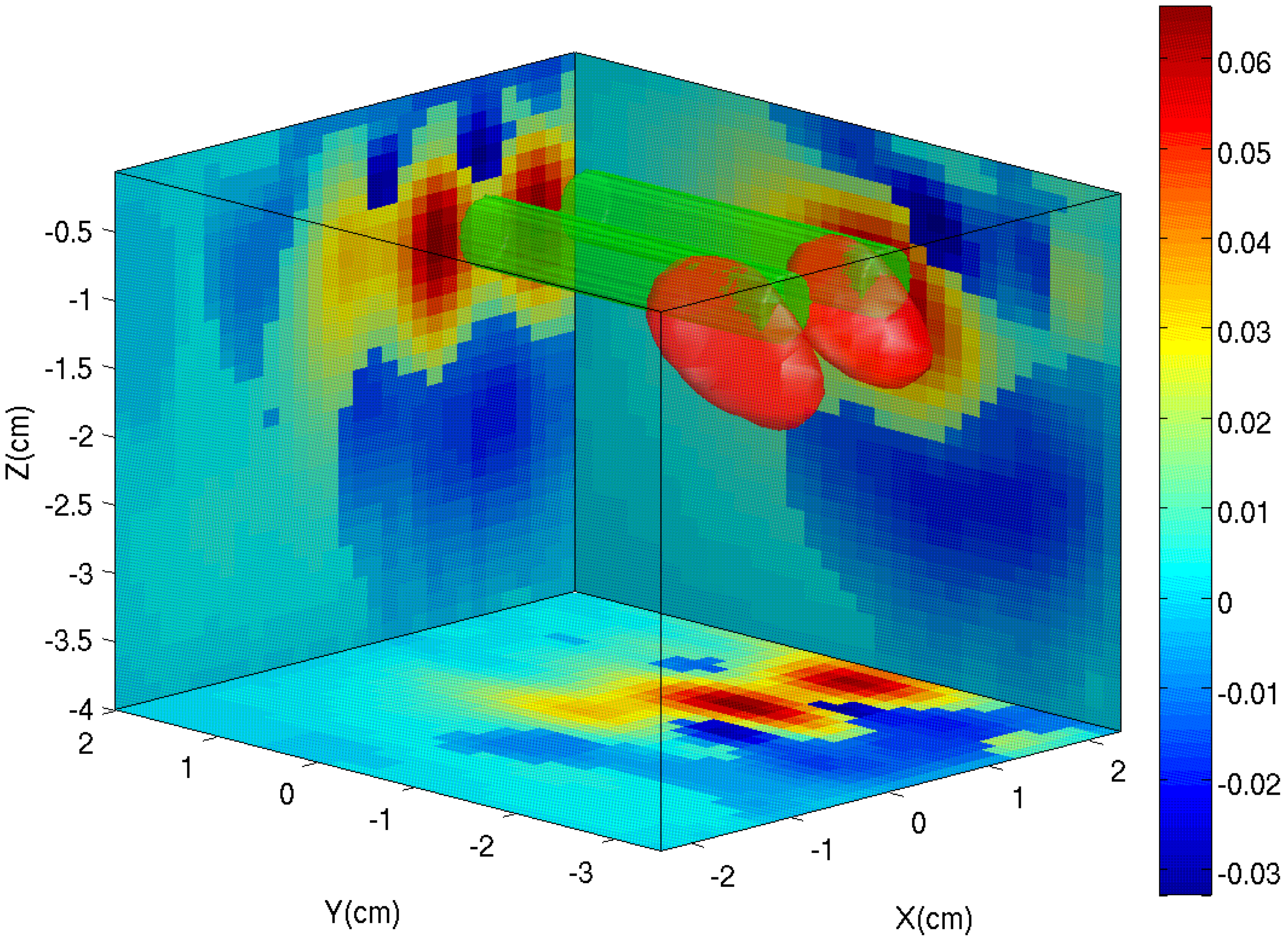

Summary & Outlook

- SPADs imagers make possible time-resolved high spatial resolution measurements for 3D NIRI

  ✓ Design a NIRI system based on a SPAD image sensor

  ✓ Develop the image reconstruction algorithm

  ✓ Build the system

  ➔ Performance evaluation

  - Design a new SPAD image sensor
  - Pre-clinical trials

Thanks to

Oliver Sieber
Thomas Mühlemann
Martin Biallas
Andreas Metz
Damien de Courten
Felix Scholkmann
Sonja Spichtig
Ivo Trajkovic
Daniel Ostojic
Christoph Kuhn
Hans-Ulrich Bucher
Dominik Marti
Martin Frenz

Questions ?

ÉCOLE POLYTECHNIQUE FÉDÉRALE DE LAUSANNE

BORL Biomedical Optics Research Laboratory
University Hospital Zurich | Clinic of Neonatology

UniversitätsSpital Zürich
Dept. Frauenheilkunde
Klinik für Neonatologie

Outline

- Introduction
- Imaging system
- Image reconstruction
- Preliminary results

Absorption

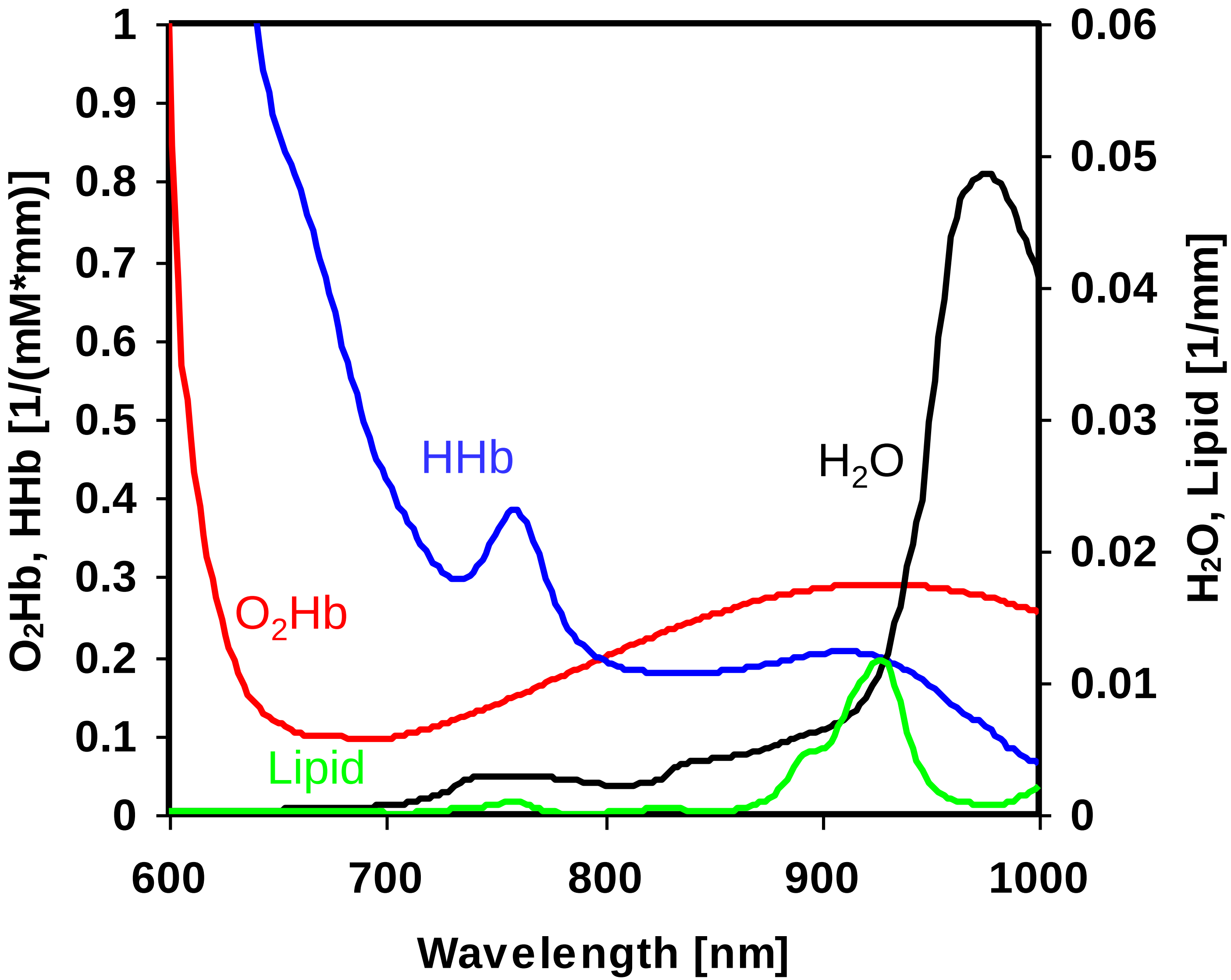

1
0.9
0.8
0.7
0.6
0.5
0.4
0.3
0.2
0.1
0
O2Hb, HHb [1/(mM*mm)]
0.06
0.05
0.04
0.03
0.02
0.01
0
H2O, Lipid [1/mm]
HHb
H2O
O2Hb
Lipid
600
700
800
900
1000
Wavelength [nm]

Experimental Techniques

Continuous wave (CW)

Frequency domain (FD)

Time domain (TD)

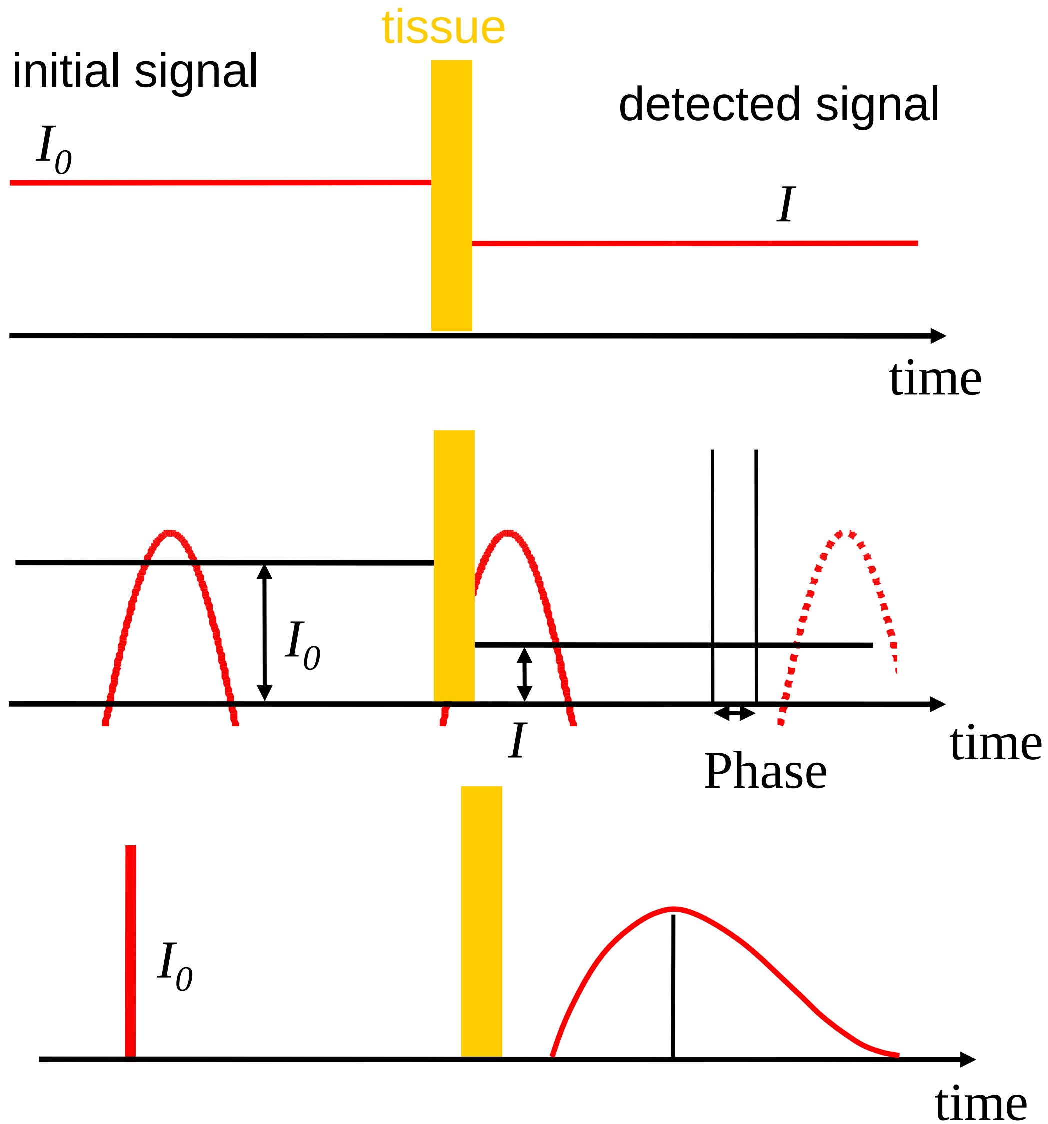

Scattering

- Random walk theory
- Photon random walk step in biological tissue ~1mm

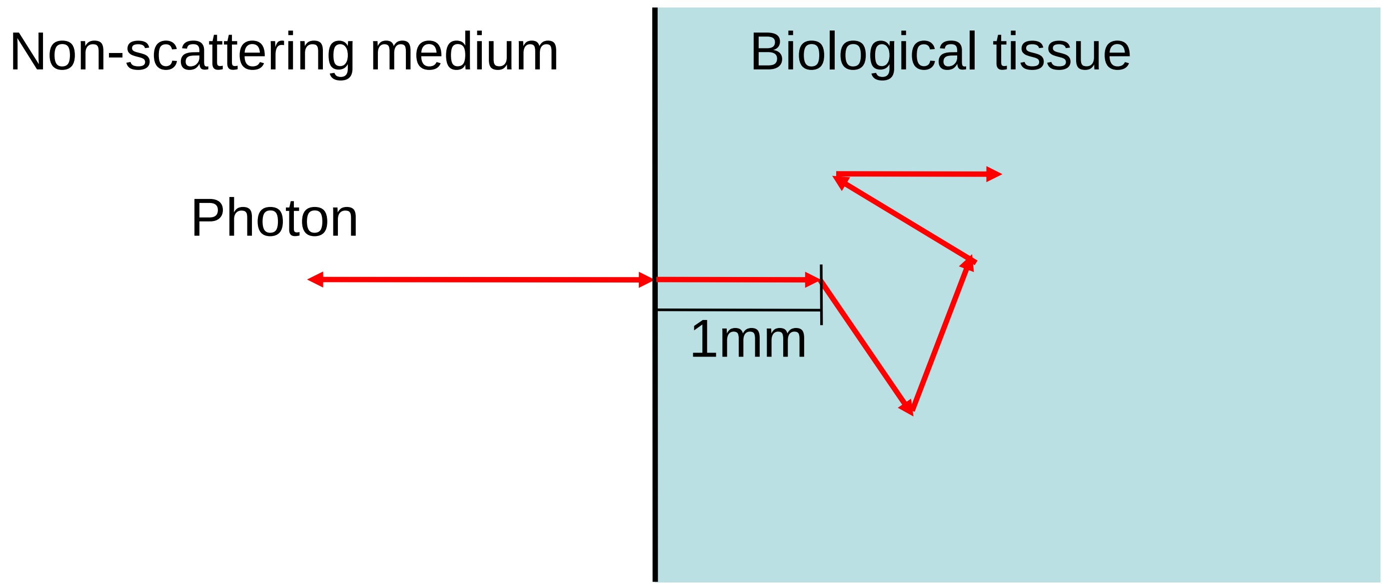

Time Correlated Single Photon Counting (TCSPC)

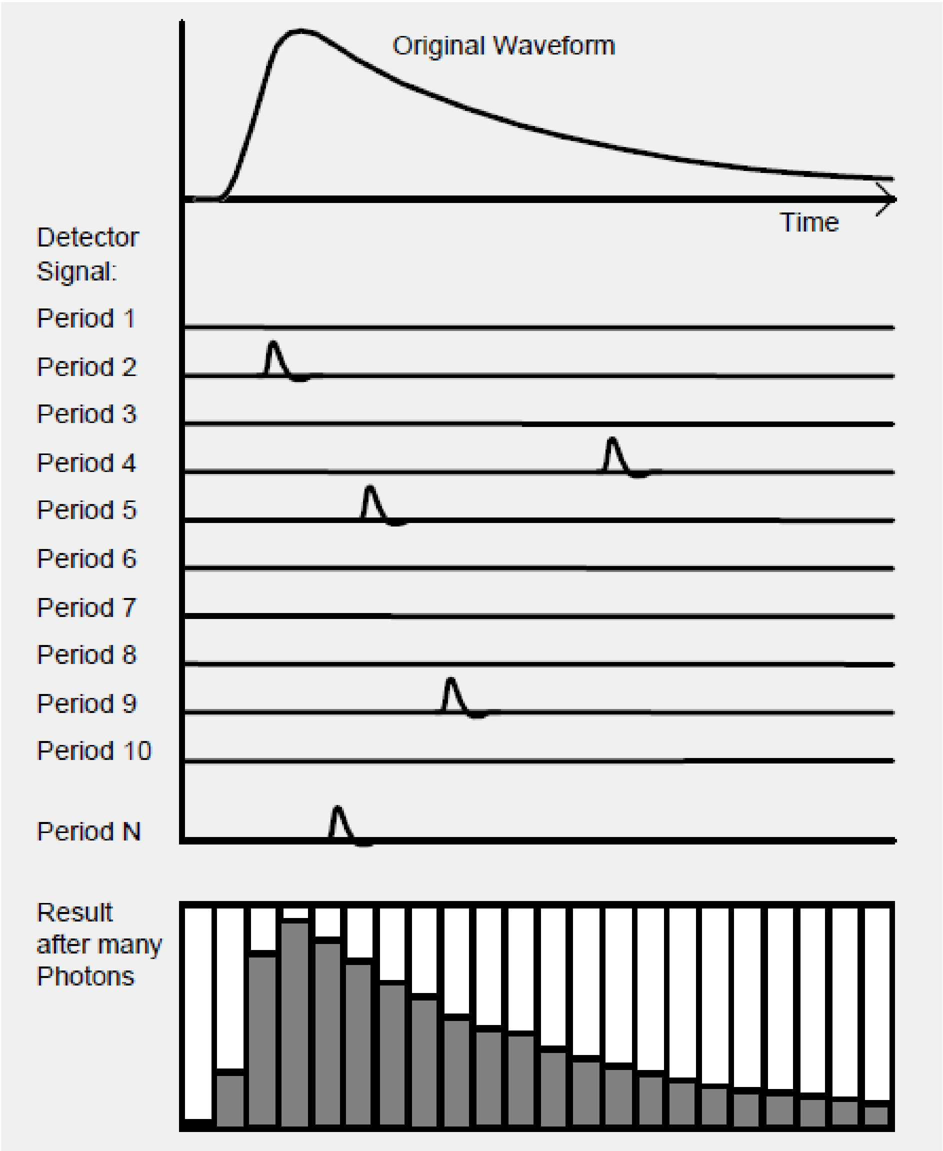

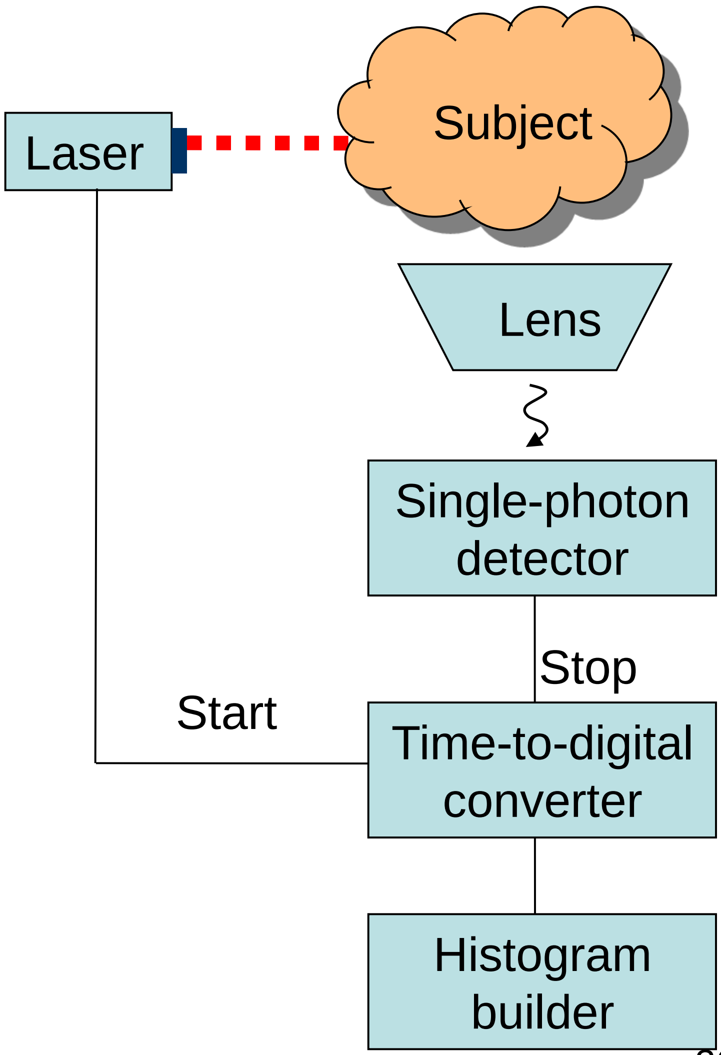

Applications

- Perfusion state of tissue
- Tissue oxygenation monitoring
- Internal bleeding
- Detection of infarcts
- Tumor detection and analysis
- Viability of tissue
- Tissue function

SPAD Image Sensor: LASP Chip

- CMOS 0.35µm technology
- 3.2mm x 3.2mm active area
- Fill factor 6%
- Microlenses improve the fill factor up to 50%

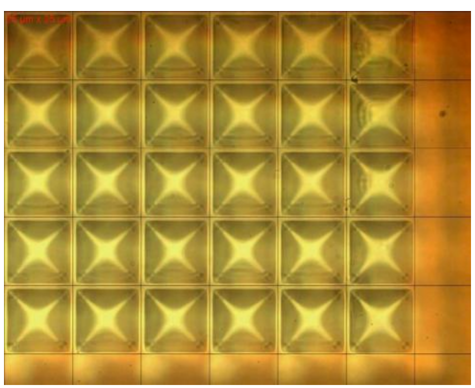

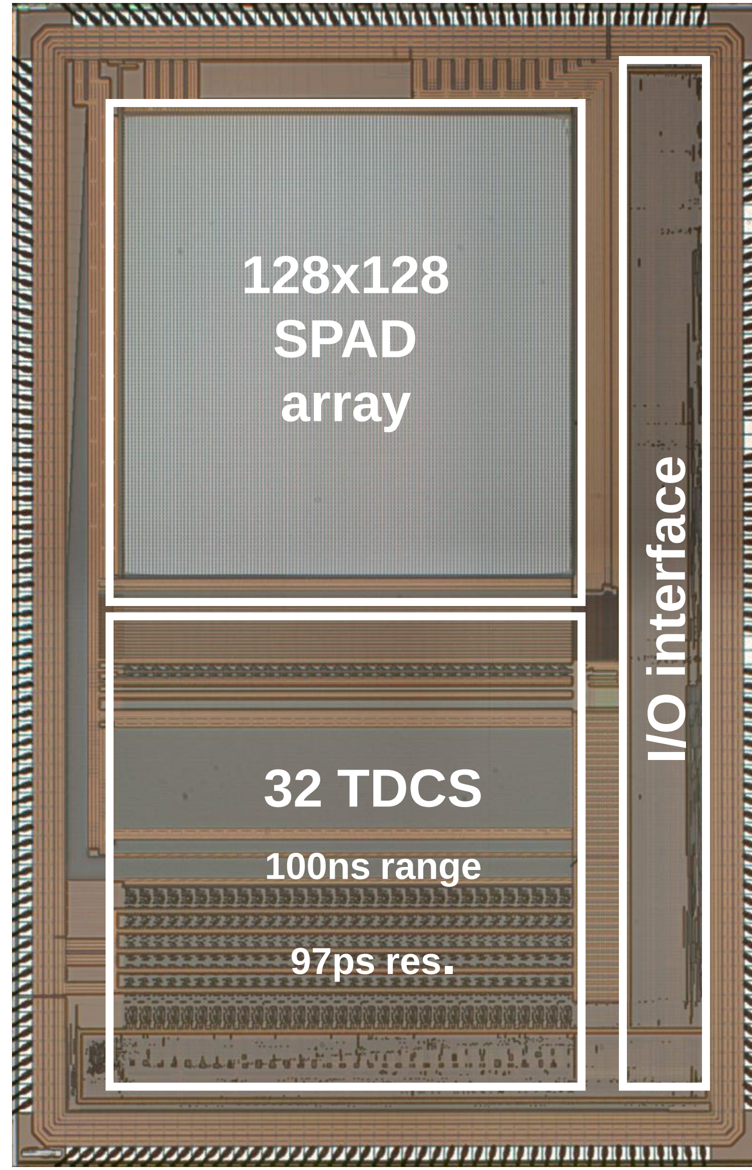

[Niclass et al JSSC 2008]

SPAD Image Sensor Architecture

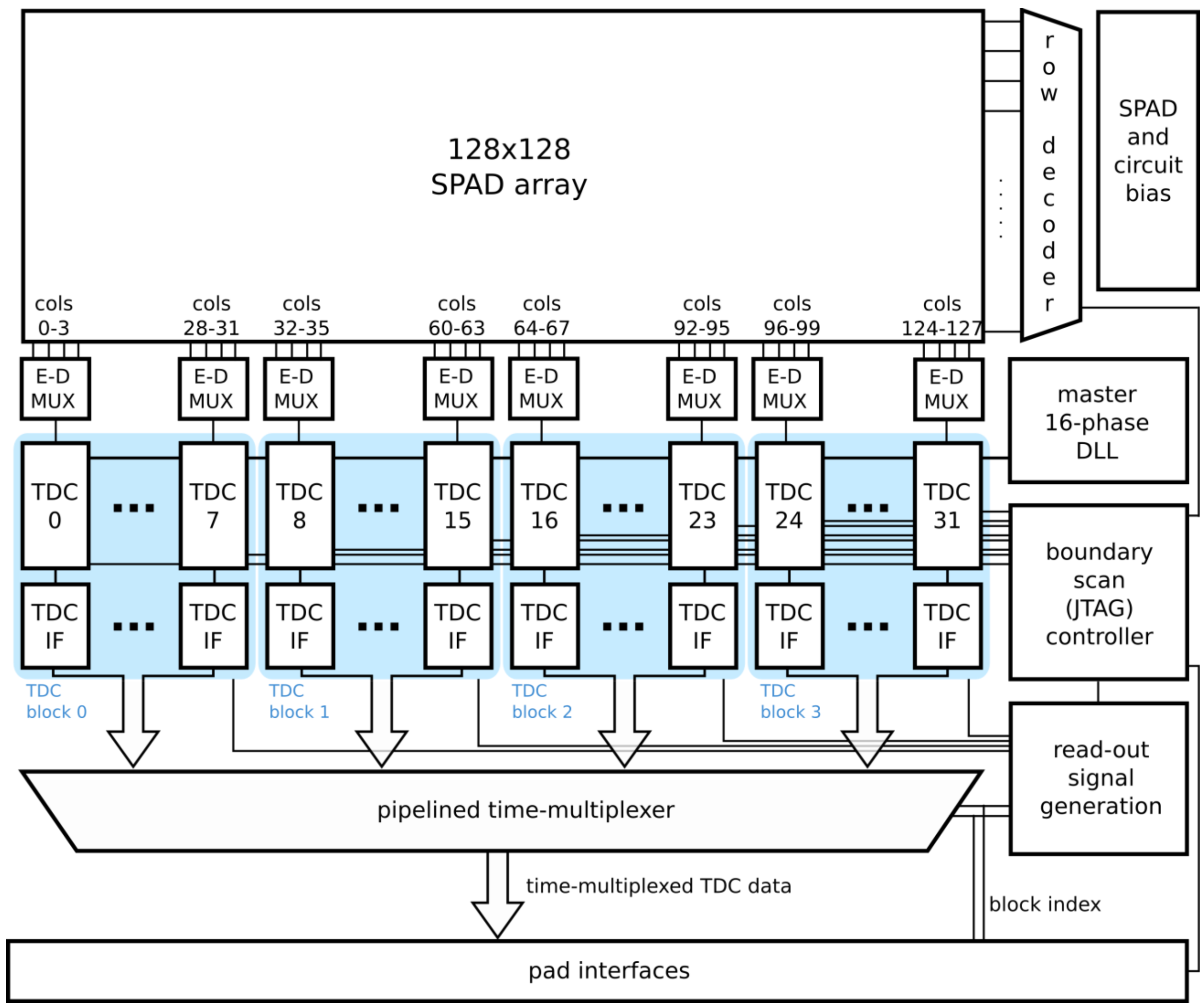

[Niclass et al JSSC 2008]

Laser: Becker & Hickl BHL-700

- 780nm wavelength
- Repetition rate 80MHz (fixed)
- Pulse width ~100ps at 1mW
- 0.2mW to 10mW adjustable average CW power
- 300mW typical peak power

[www.becker-hickl.de]

Experimental Setup with Cylindrical Waves I

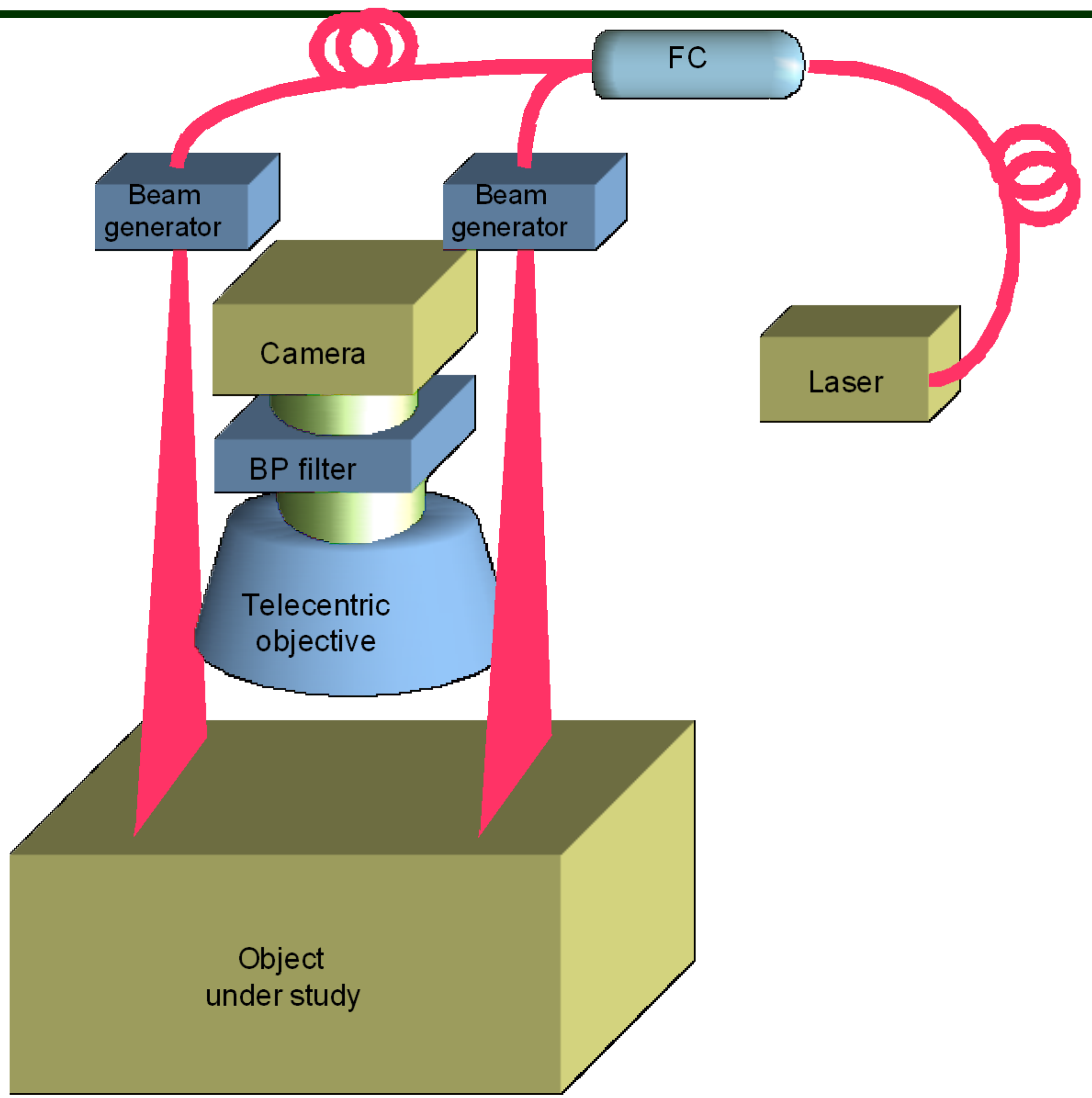

Trigger Adaptation Circuit

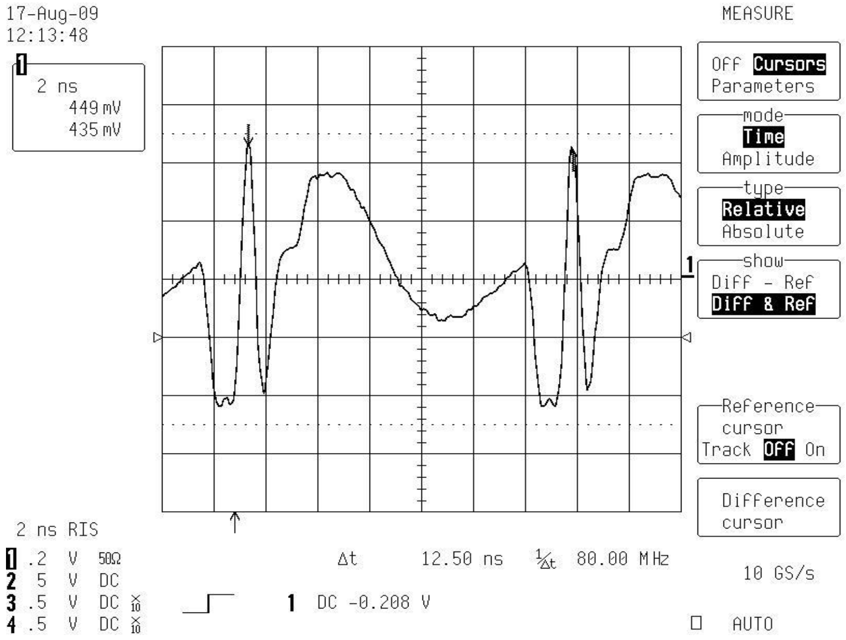

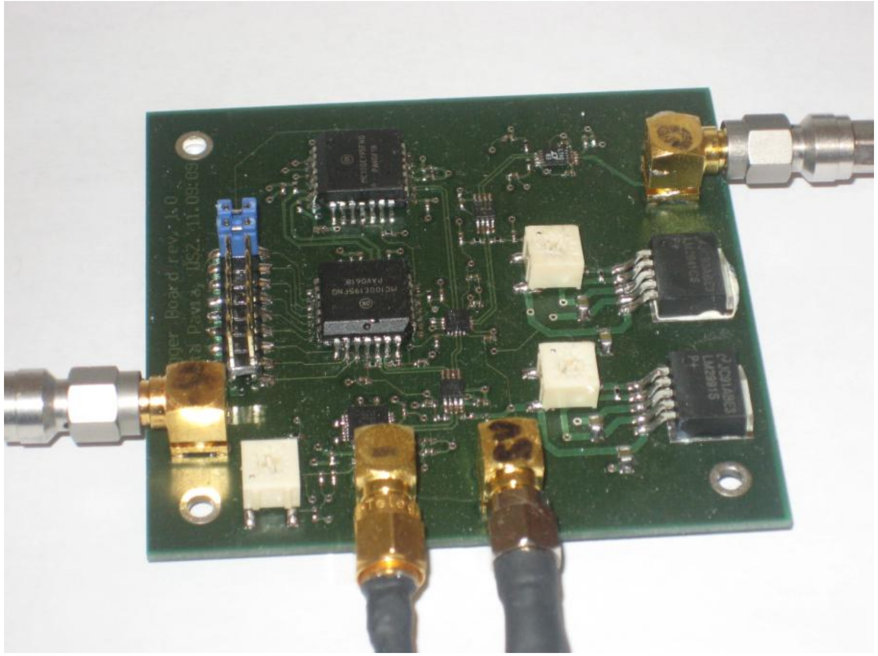

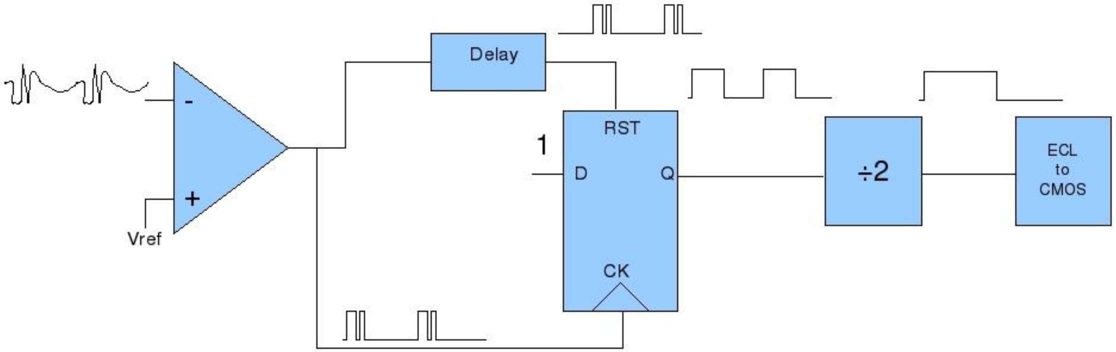

Experimental Setup with Plane Waves

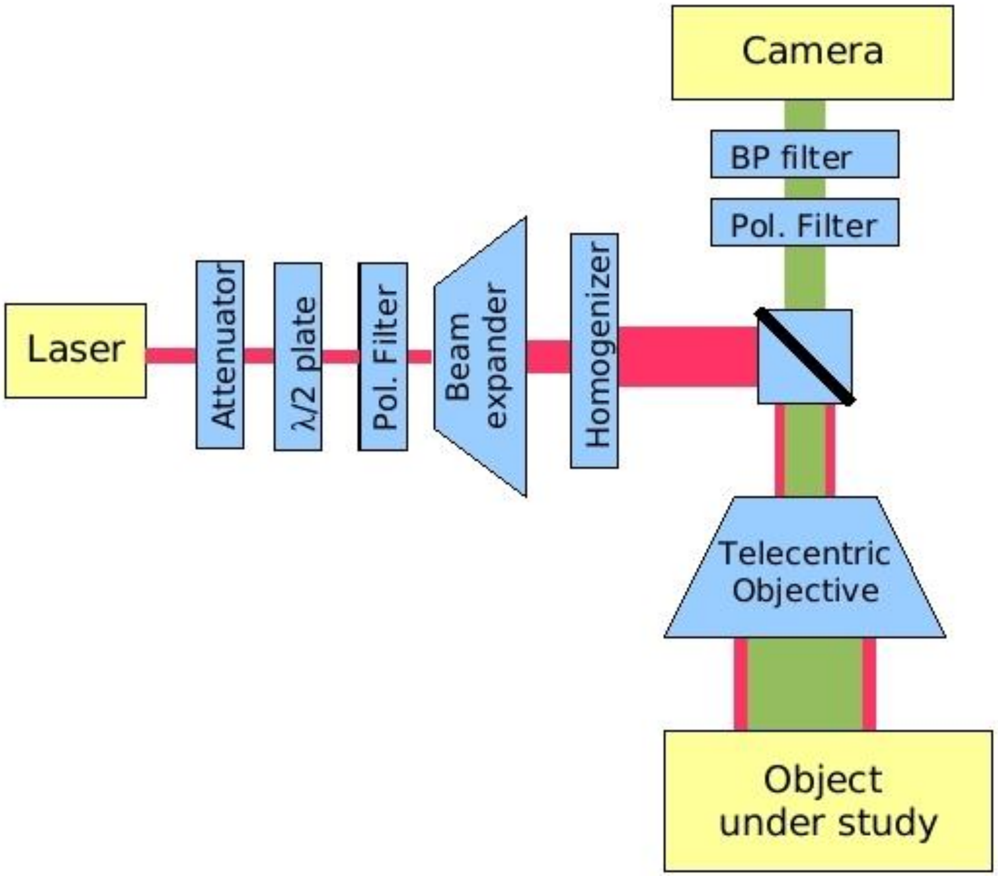

Results with Plane Waves

- SPAD's Impulse Response Function (IRF) is too slow

- Time gating-window (GW) does not improve the IRF

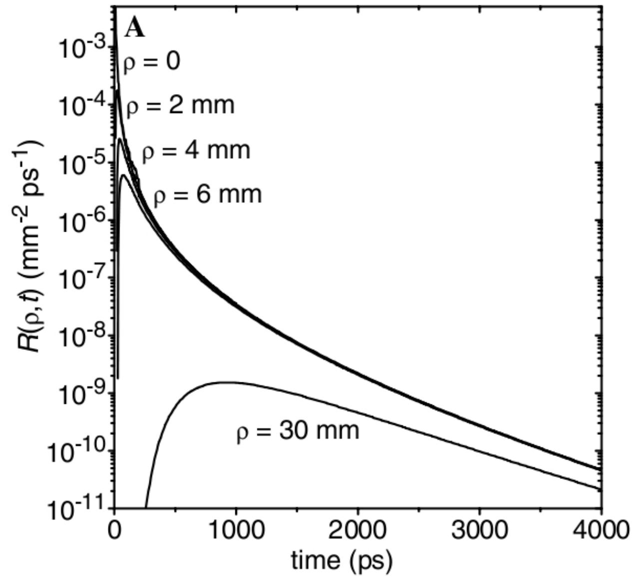

[Torricelli et al. 2005]

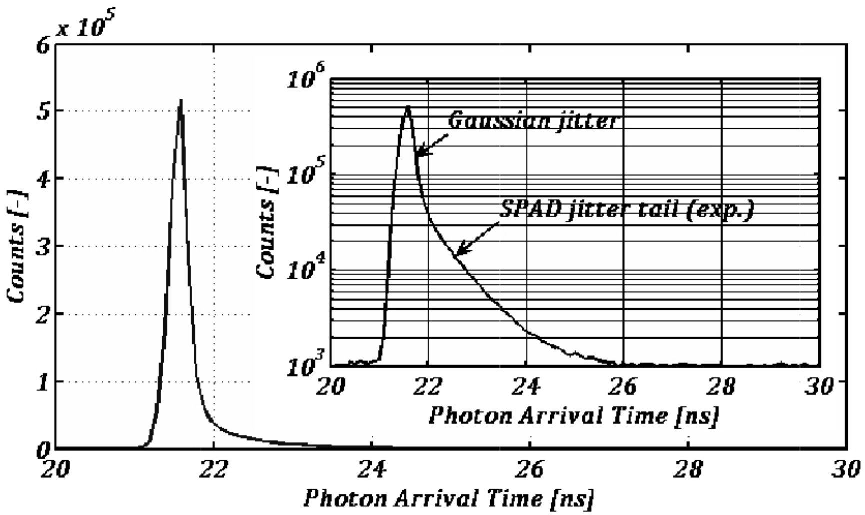

[Niclass C et al JSSC 2008]

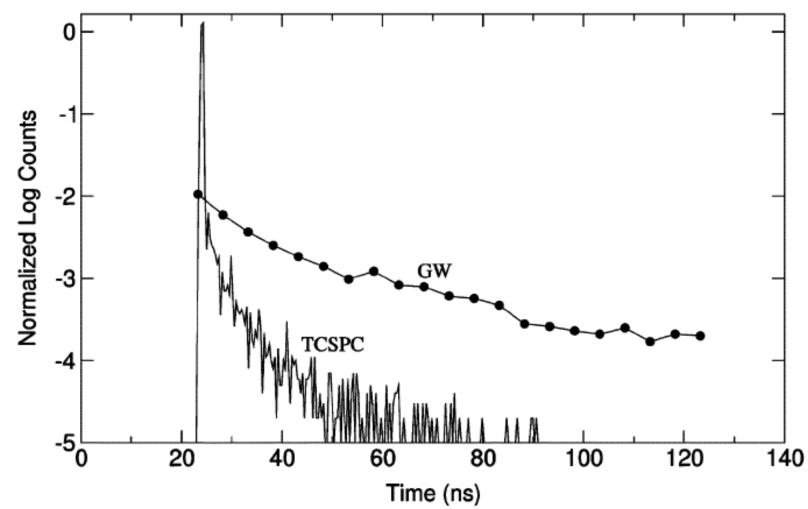

[Schwartz D et al JSSC 2008]

Time-to-digital Converter Linearity

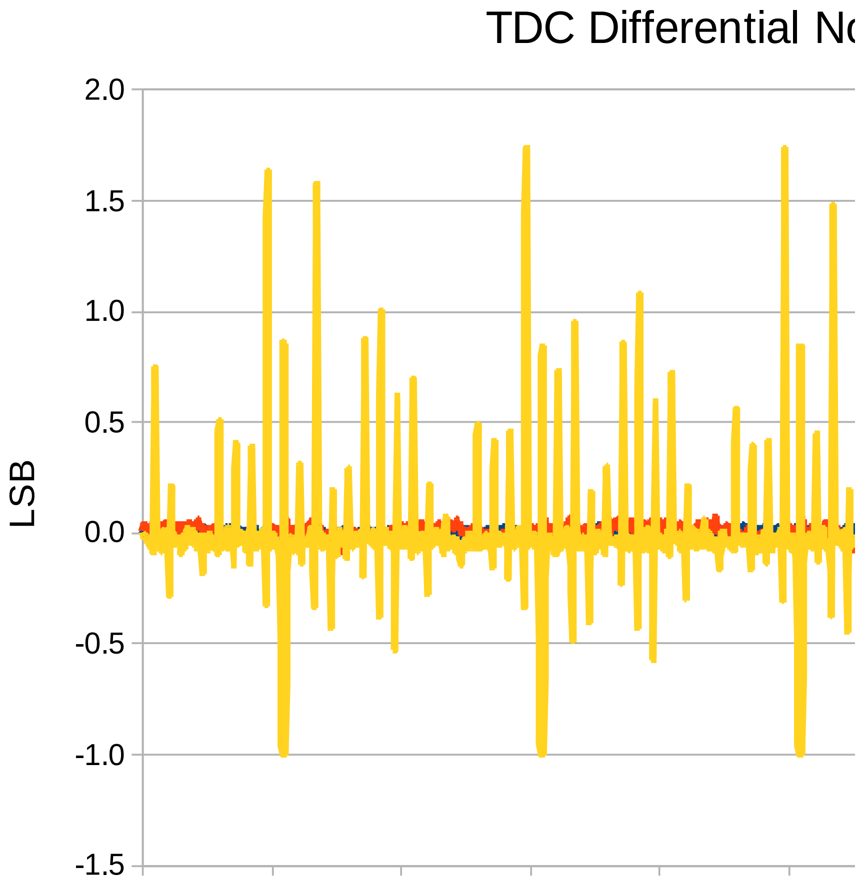

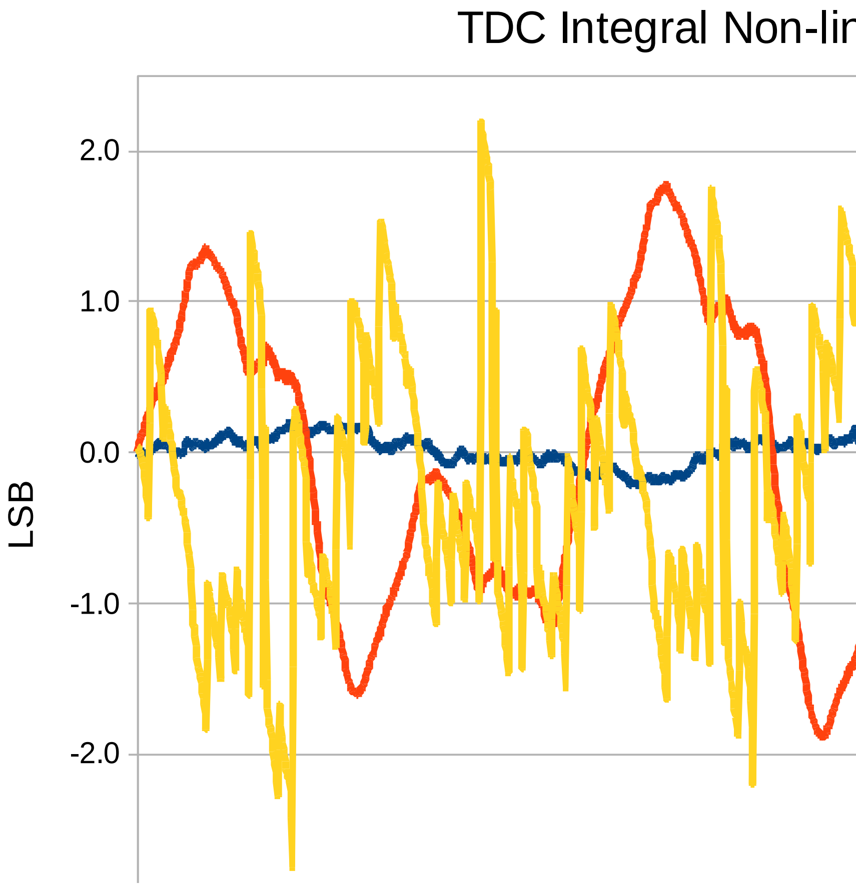

Detector: Photon Detection Probability (PDP)

- PDP increases with the excess bias voltage, but so does the DCR.
- The shallow p+ / n-well junction explains why the SPAD is more effective at blue/UV wavelengths than at red/IR.

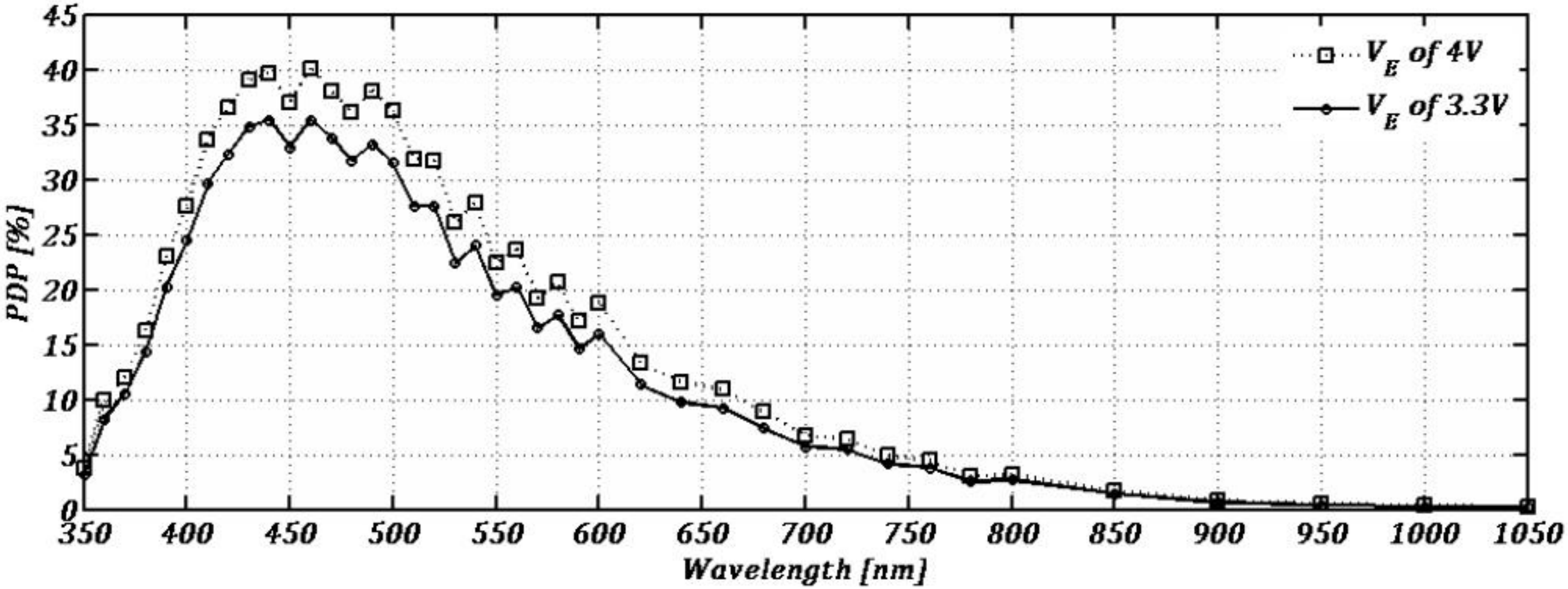

[Niclass C et al JSSC 2008]

Dark Count Rate (DCR)

- Pulses generated in the SPAD in the absence of light.
- Causes:
  - Thermal generation of carriers
  - Electron-hole generation due to tunneling effects.

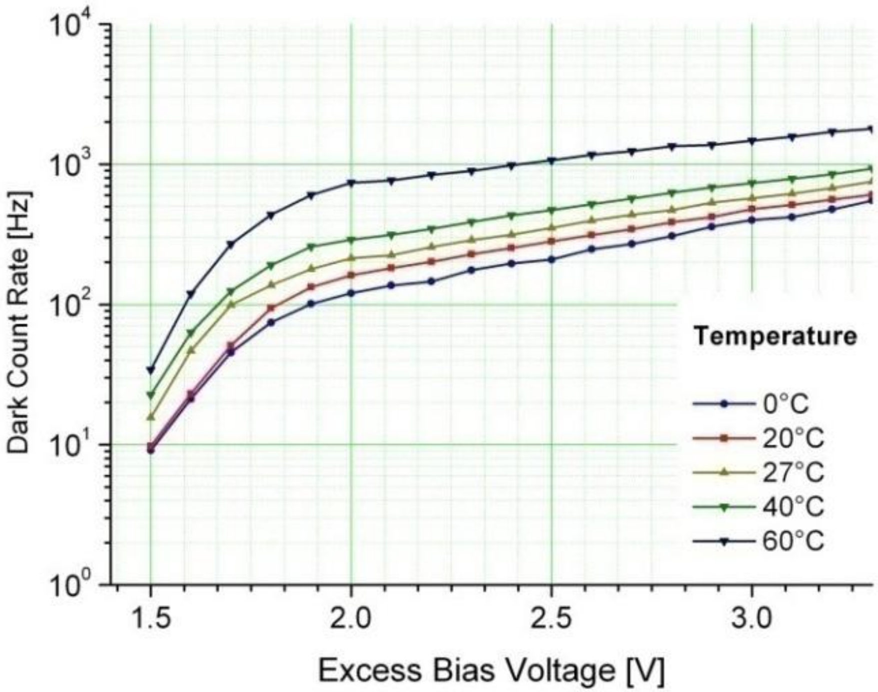

[Niclass C et al JSSC 2008]

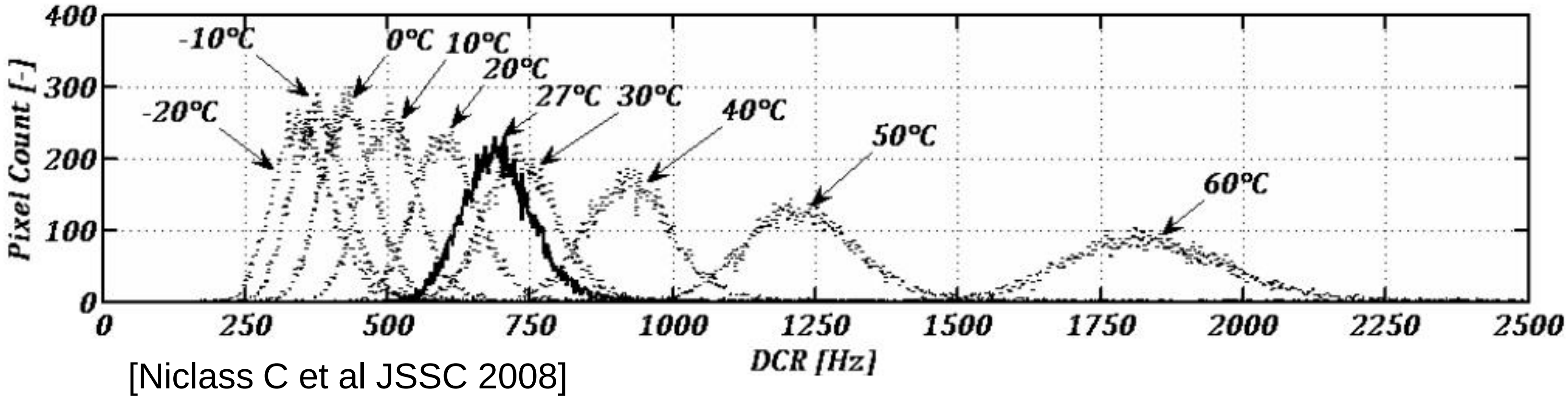

[Niclass C et al JSSC 2008]

BHP-700 time response

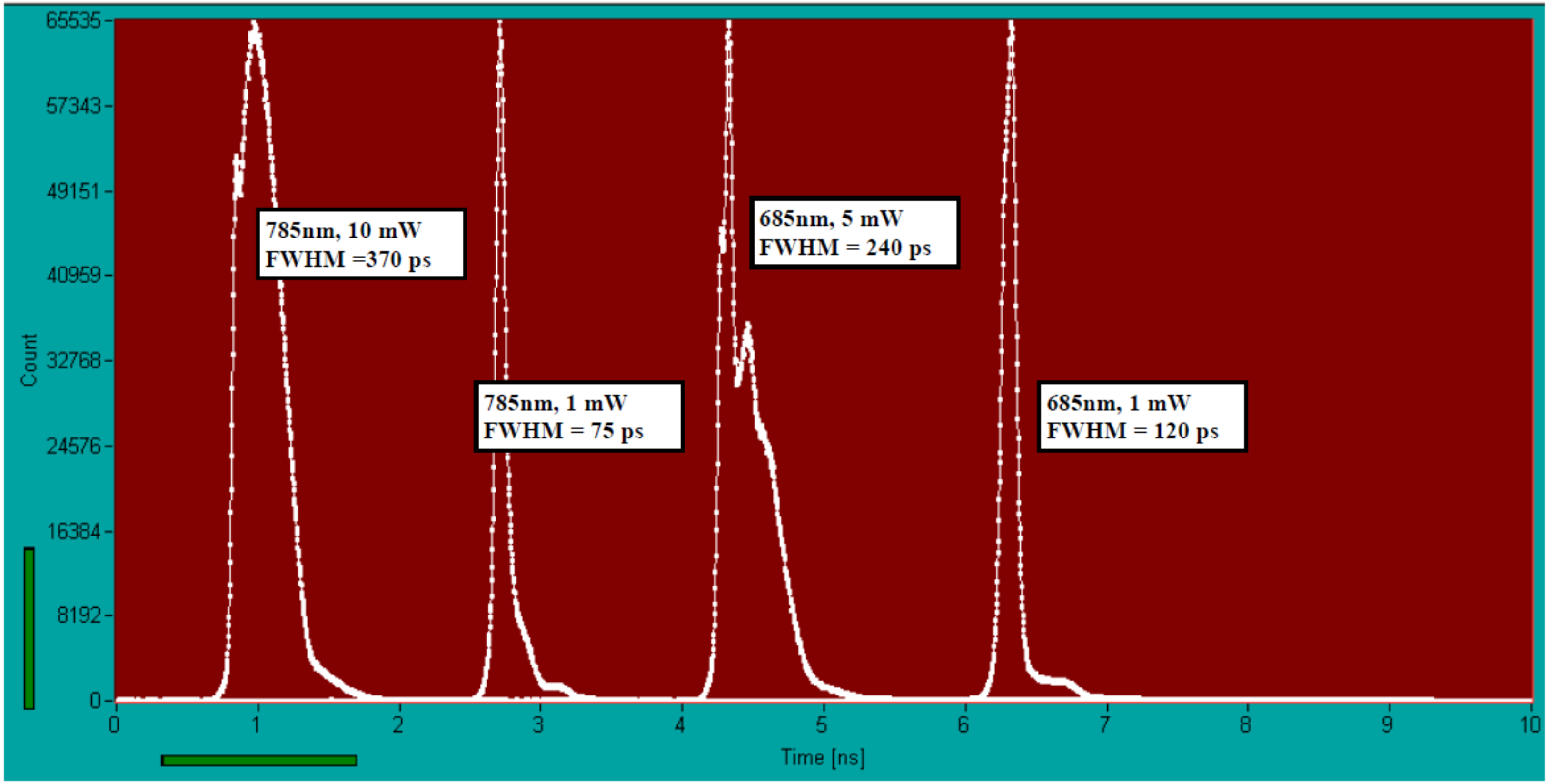

The Diffusion Equation

$$\frac{\partial U(\vec{r},t)}{\partial t} + \upsilon \mu_a U(\vec{r},t) + \nabla \cdot \vec{J}(\vec{r},t) = q(\vec{r},t)$$

$$\nabla U(\vec{r},t) + \frac{3\partial \vec{J}(\vec{r},t)}{\upsilon^2 \partial t} + \frac{\vec{J}(\vec{r},t)}{D} = 0$$

$$D = \frac{\upsilon}{3\mu_s'}$$

$U(\vec{r},t) : photon\ density\ wave$

$\vec{J}(\vec{r},t) : photon\ density\ current$

$\upsilon : speed\ of\ light$

$\mu_a : absorption\ coefficient$

$\mu_s' : reduced\ scattering\ coefficient$

$D : diffusion\ coefficient$

$q(\vec{r},t) : source\ term$

- Homogeneous medium
- Fourier in the time domain

$$\nabla^2 U(\vec{r},\omega_t) + k^2 U(\vec{r},\omega_t) = -\frac{q(\vec{r},\omega_t)}{D}$$

$$k^2 = \frac{(-\upsilon\mu_a - i\omega_t)}{D}$$

Using the first Born approximation

$$\mu_a(\vec{r}) = \mu_a^0 + \mu_a^s(\vec{r}) \qquad U(\vec{r}) = U_0(\vec{r}) + U_s(\vec{r})$$

$$(\nabla^2 + k^2)U_s(\vec{r}) = \frac{\upsilon\mu_a^s(\vec{r})}{D}(U_0(\vec{r}) + U_s(\vec{r}))$$

Object to be reconstructed

$$U_s(\vec{r}) = -\int g(\vec{r}|\vec{r}')\frac{\upsilon\mu_a^s(\vec{r}')}{D}U_0(\vec{r}')d\vec{r}'$$

Measurement

Matrix coefficients

The Diffusion Equation for Plane Waves

Fourier in XY dimensions

$$\left(\frac{\partial^2}{\partial z^2} + (k^2 - \omega_x^2 - \omega_y^2\right) U_s(\omega_x, \omega_y, z) = \mathcal{F}_{xy}\left\{\frac{\upsilon\mu_a^s(\vec{r}')}{D} U_0(\vec{r}')\right\}$$

$$\gamma_{xy}^2 = \omega_x^2 + \omega_y^2 - k^2$$

Infinite medium

$$U_s(\omega_x, \omega_y, z) = -\int \mathcal{F}_{xy}\left\{\frac{\upsilon\mu_a^s(\vec{r}')}{D} U_0(\vec{r}')\right\} \frac{e^{-\gamma_{xy}|z-z'|}}{2\gamma_{xy}} dz'$$

Homogeneous field is XY independent

$$U_s(\omega_x, \omega_y, z) = -\frac{ie^{-\gamma_{xy}z + ikz_0}}{4Dk\gamma_{xy}} \int O(\omega_x, \omega_y, z') e^{(\gamma_{xy} - ik)z'} dz'; o(\vec{r}) = \frac{\upsilon\mu_a^s(\vec{r}')}{D}$$

The Diffusion Equation for Cylindrical Waves

Fourier in the X dimension

$$\Big(\frac{\partial^2}{\partial z^2} + \frac{\partial^2}{\partial x^2} + (k^2 - \omega_x^2\Big) U_s(\omega_x, y, z) = \mathcal{F}_x\Big\{\frac{\upsilon\mu_a^s(\vec{r}')}{D} U_0(\vec{r}')\Big\}$$

$$\gamma_x^2 = \omega_x^2 - k^2$$

Infinite medium

$$U_s(\omega_x, y, z) = -\iint \mathcal{F}_x\Big\{\frac{\upsilon\mu_a^s(\vec{r}')}{D} U_0(\vec{r}')\Big\}\frac{i}{4} H_0^{(1)}(i\gamma_x|\vec{r}'_{yz} - \vec{r}^{\,0}_{yz}|)dy'dz'$$

Homogeneous field is X independent

$$U_s(\omega_x, y, z) = -\iint O(\omega_x, y', z')\frac{i}{4D} H_0^{(1)}(k|\vec{r}'_{yz} - \vec{r}^{\,0}_{yz}|)\frac{i}{4} H_0^{(1)}(i\gamma_x|\vec{r}_{yz} - \vec{r}'_{yz}|)dy'dz'$$

Reconstruction Algorithm

- **Semi-infinite medium:** the method of images can be applied
- **Multiple sources:** superposition principle
- **TD measurements:** high number of equations for only one acquisition

The Inverse Problem: Regularization

- The problem is ill-posed by its nature.
- Regularization defines restrictions in the solution's complexity: smoothness, norm …
- Tikhonov regularization: equivalent to minimize:

Matrix to be inverted

Problem's solution (object to be reconstructed)

$$\|Ax-b\|_2^2+\lambda^2\|Lx\|_2^2$$

Measurement

Linear operator

Regularization parameter

- Sub-space preconditioned LSQR (SP-LSQR):
  - Iterative method
  - Tikhonov regularization
  - Predefined sub-space of possible solutions

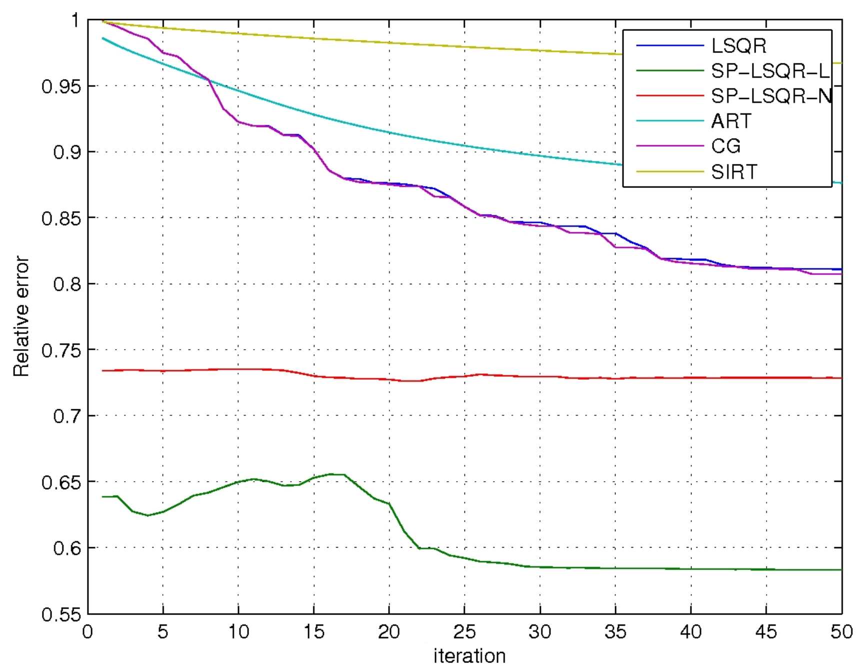

Image Reconstruction Testbench

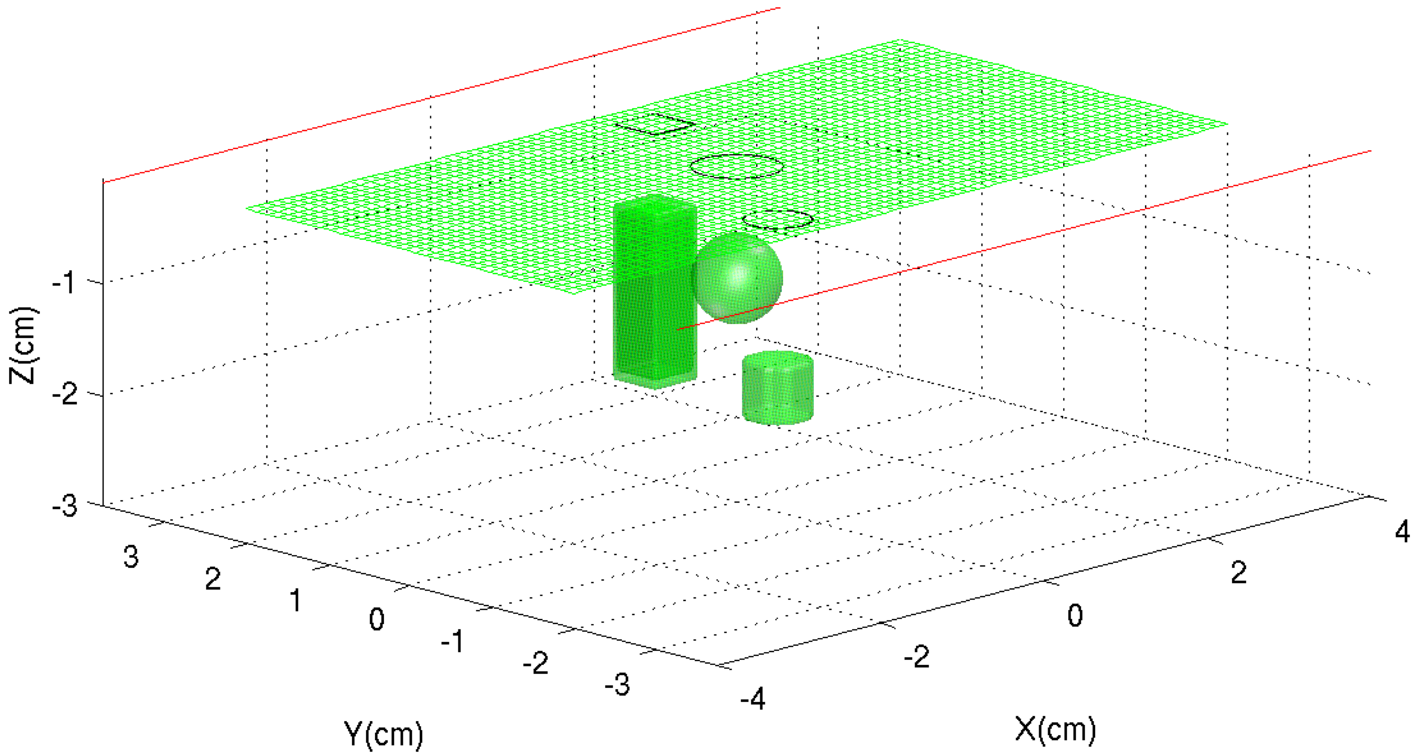

Simulation Results: ART

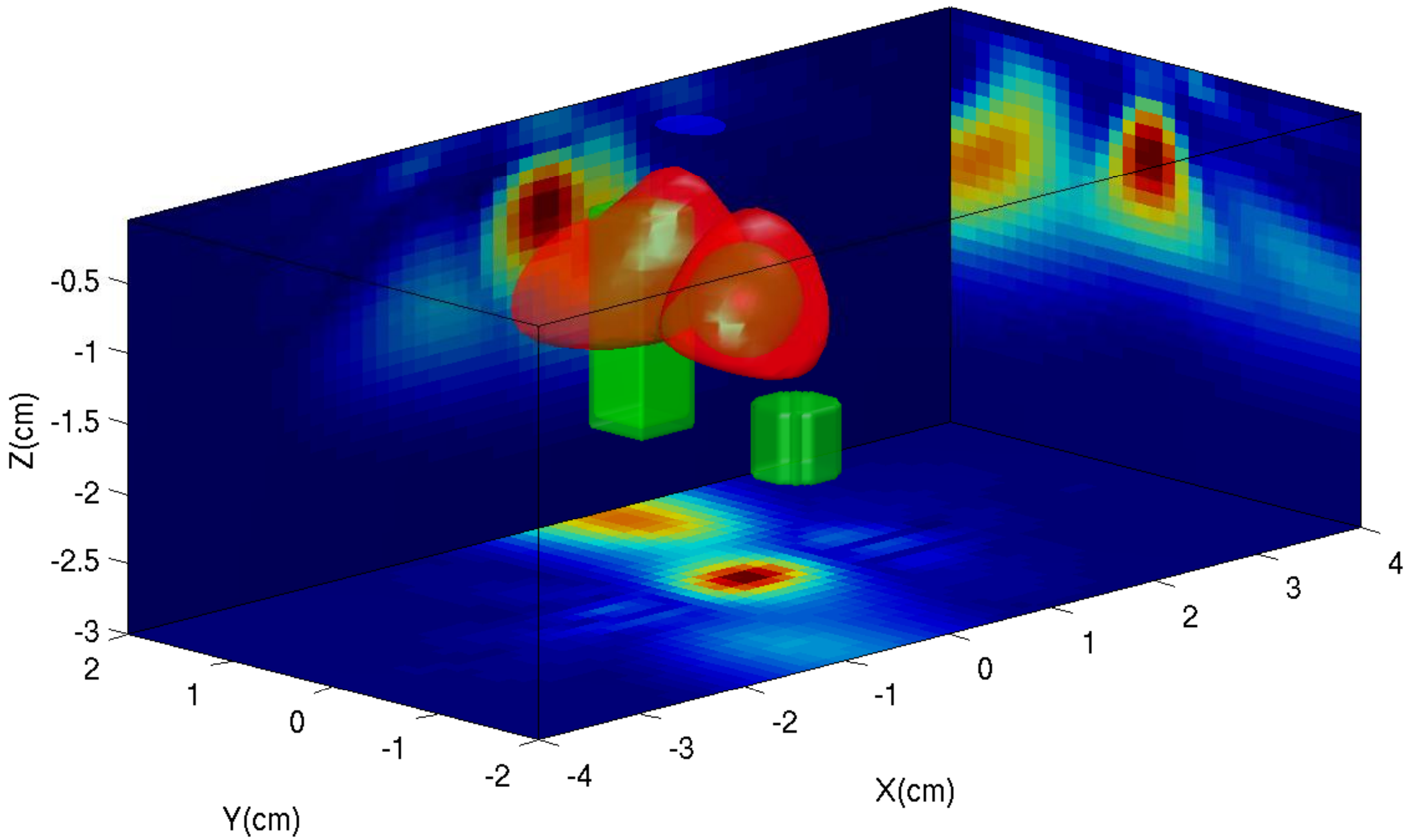

Simulation Results: LSQR

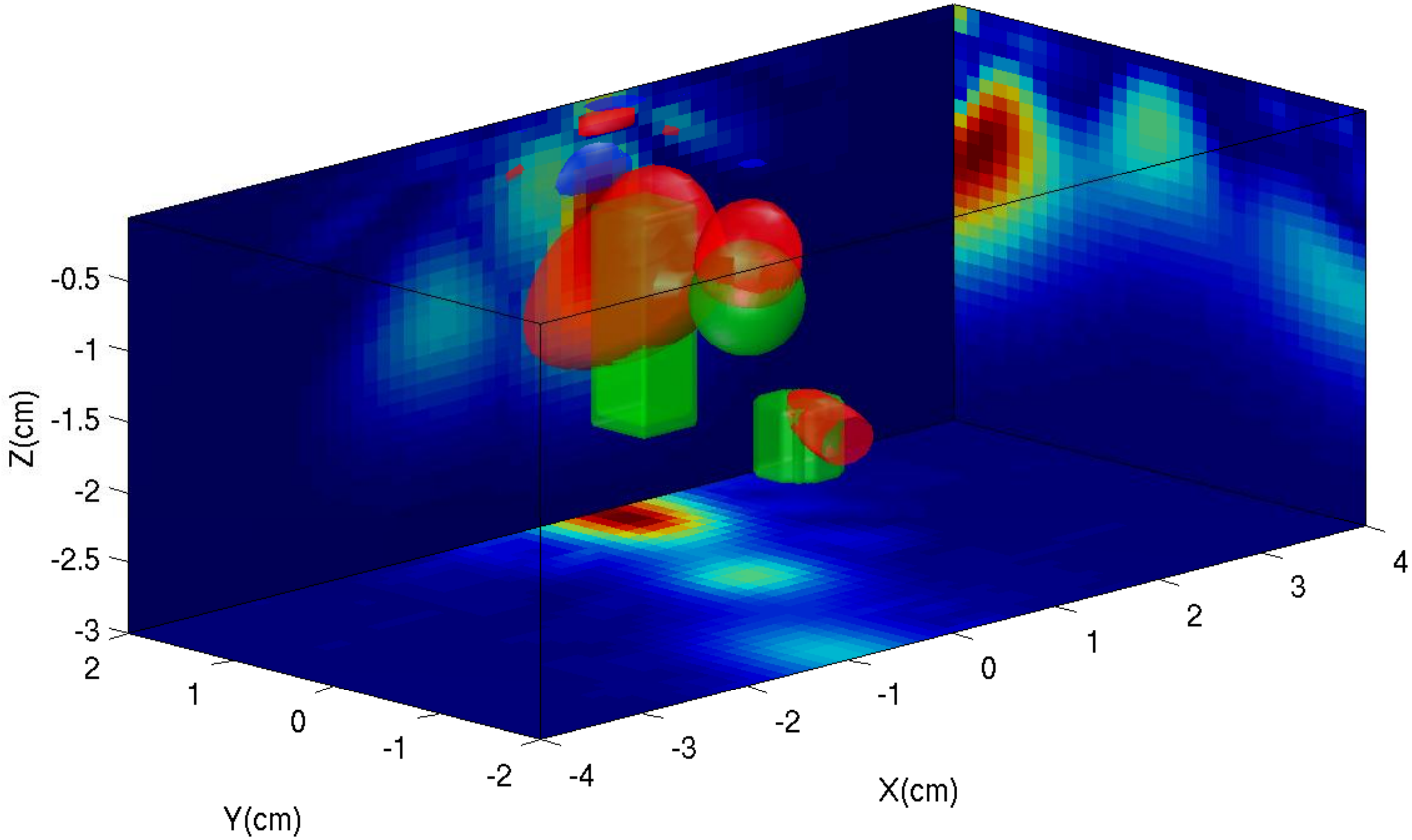

Simulation Results: SP-LSQR Norm

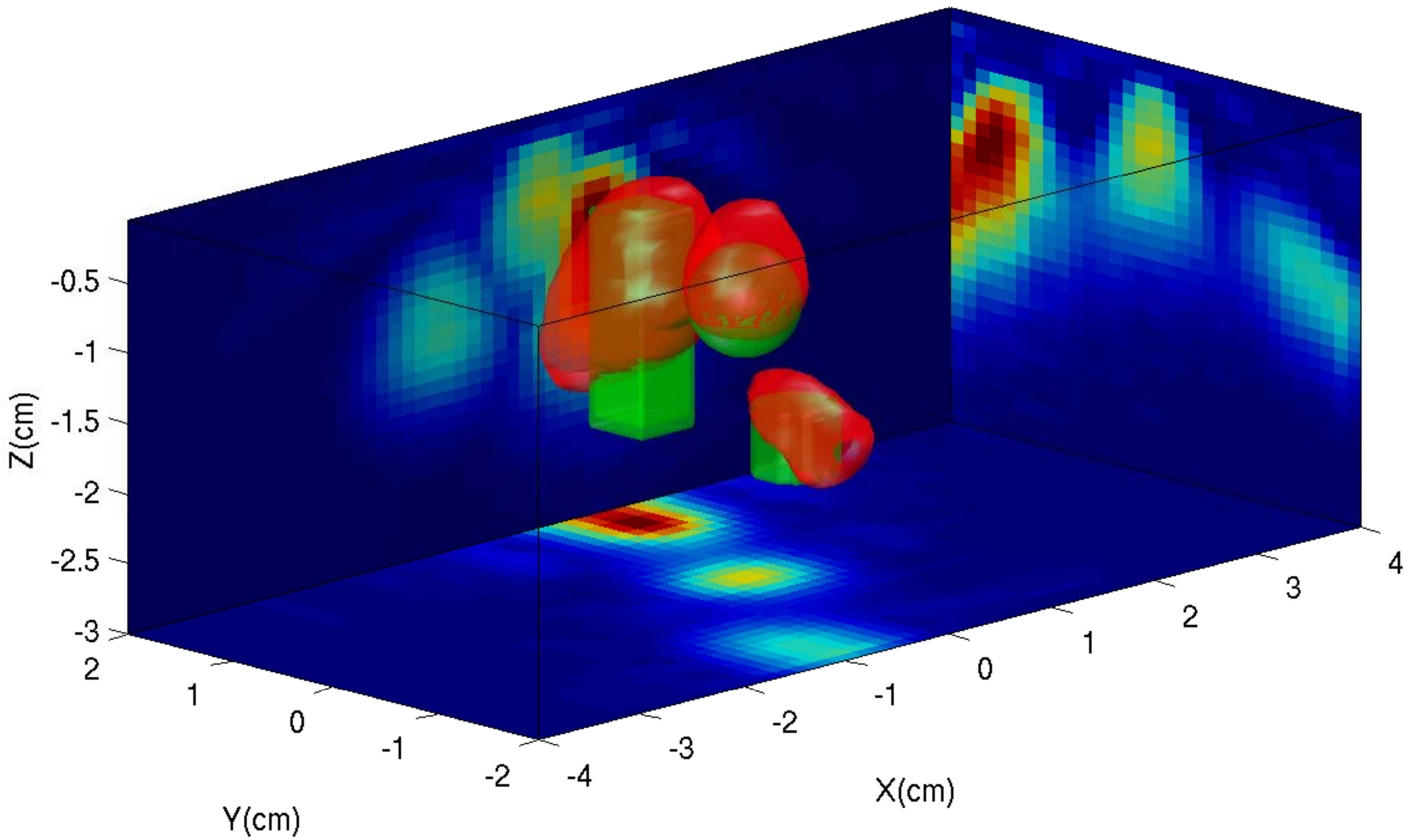

Simulation Results with SP-LSQR

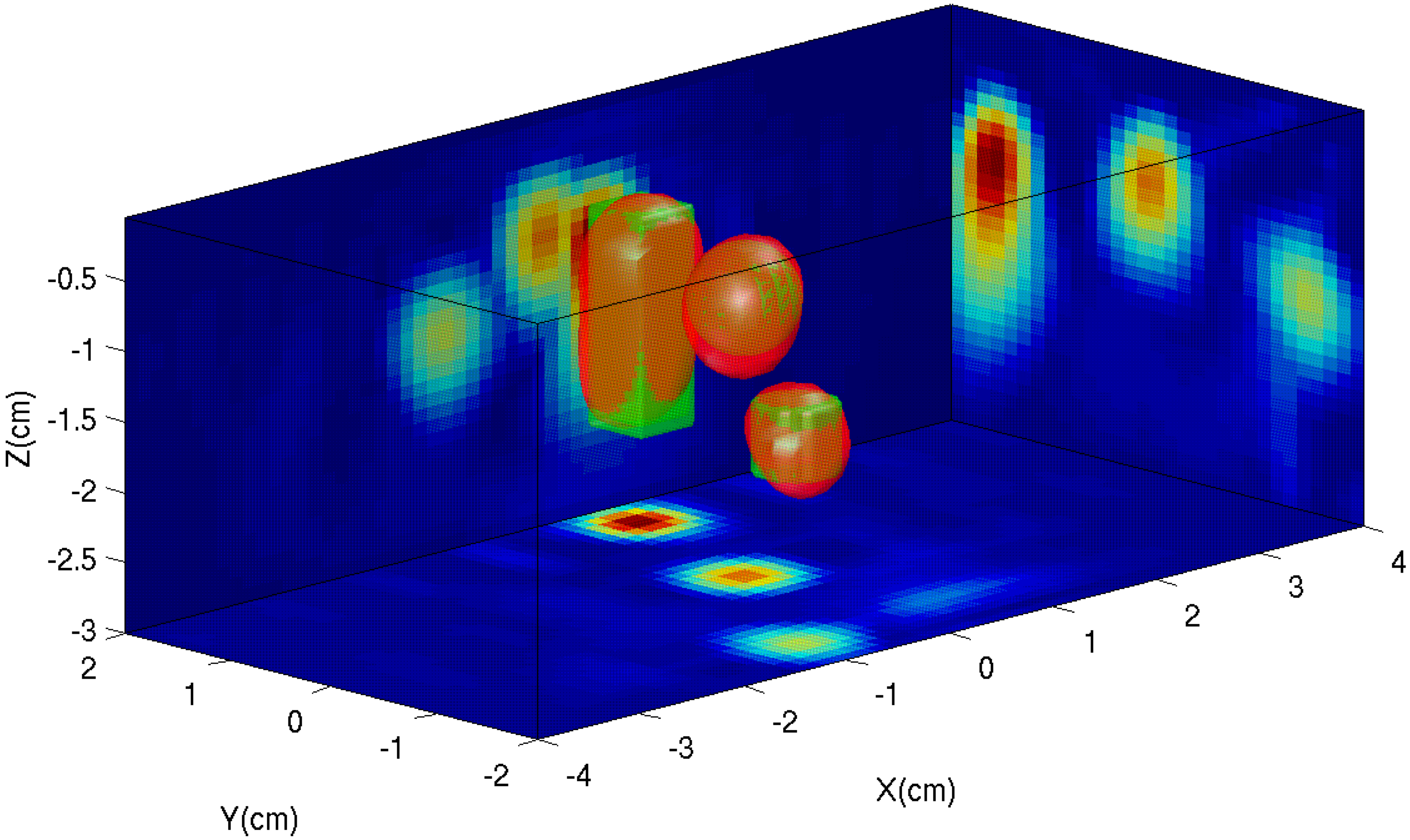

FPGA Architecture for fast data acquisition

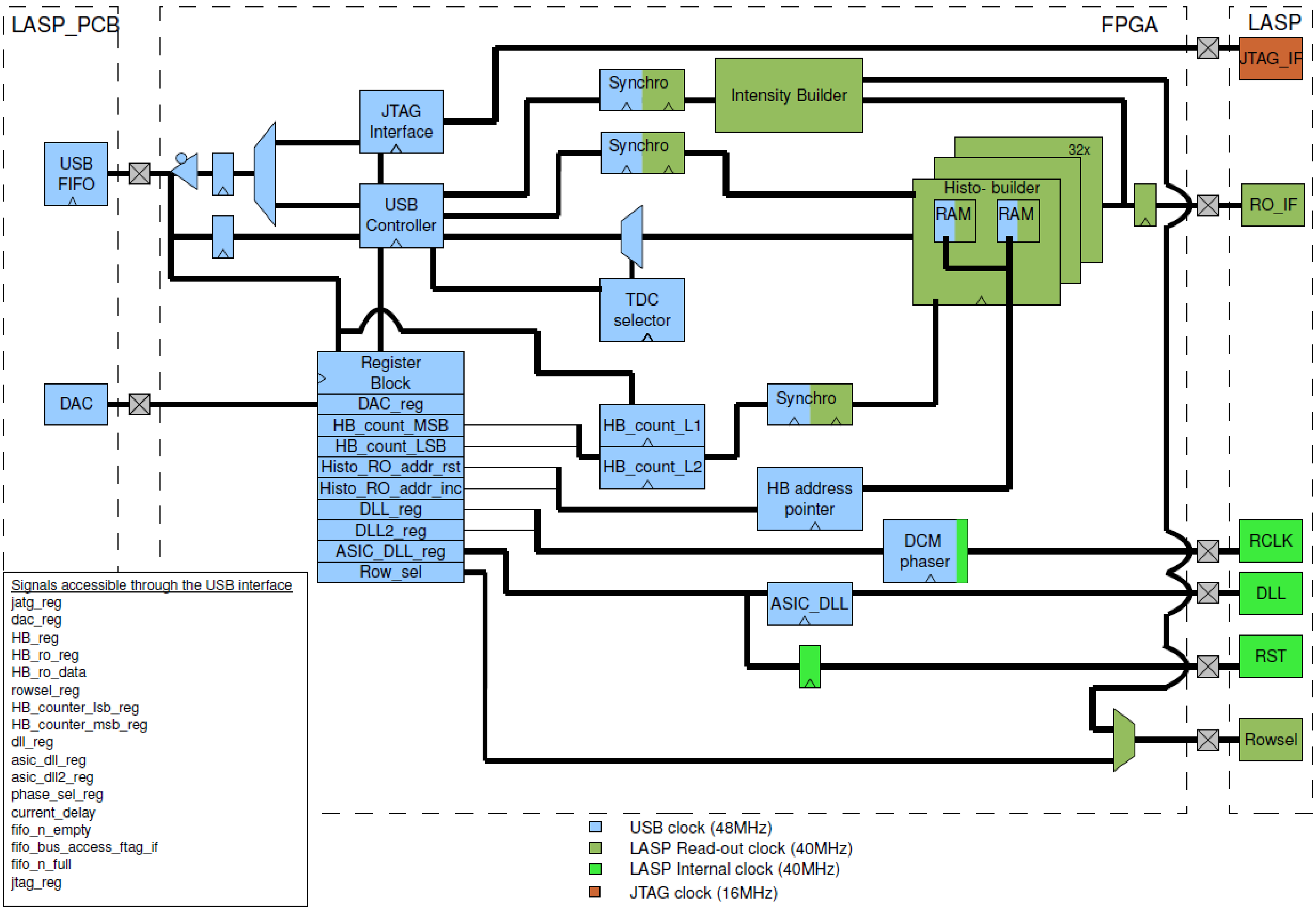

High definition imaging with NIR

- CW systems with CCD cameras.
- Long acquisition times: Full scan of the object.
- Low depth resolution.
- Only applied to small spaces. E.g. small animal imaging.

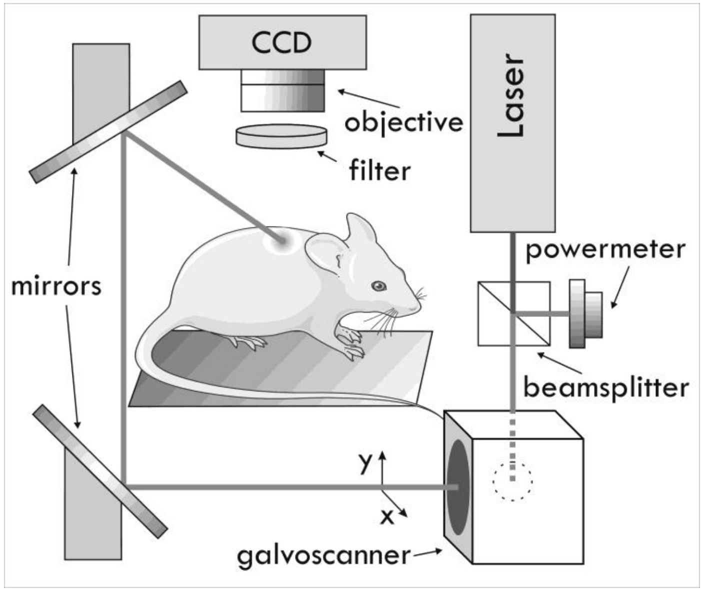

[A. Martin, Mol. Img. (2008)]

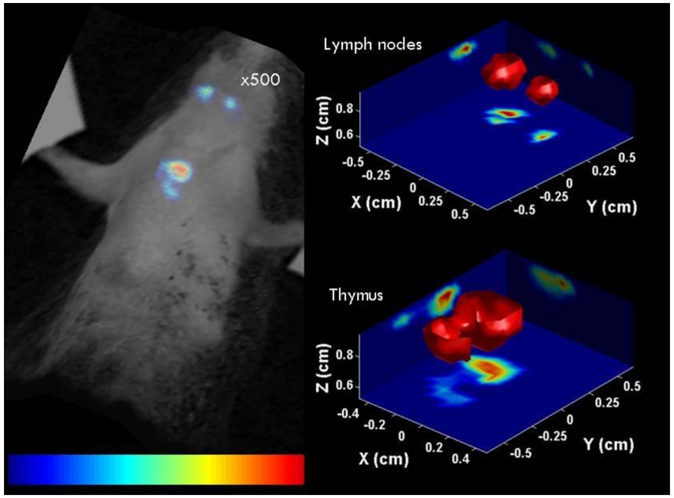

[A. Martin, Mol. Img. (2009)]

Future Modifications of the SPAD Image Sensor

- Solve the Linearity problem in the TDC
- Reduce the total time range of the TDC
- Increase the number of pixels
- Modify the TDC/pixel clustering to reduce the number of acquisitions per frame

Outlook

- ✓ Design a NIRI system based on a SPAD image sensor
- ✓ Develop an image reconstruction algorithm based on the system
- ✓ Build a system to perform measurements on phantoms
- ➔ Evaluate the performance of the new setup
- Design a customized SPAD image sensor
- Pre-clinical trials

Conclusions

- SPADs enable the acquisition of time-resolved measurements with high spatial resolution for NIRI
- They make possible the development of more efficient algorithms:
  - Higher resolution images
  - Less computation power